Exotic mesons with hidden bottom near thresholds

S. Ohkoda,[1] Y. Yamaguchi,[1] S. Yasui,[2] K. Sudoh,[3] and A. Hosaka[1]

[1]*Research Center for Nuclear Physics (RCNP), Osaka University, Ibaraki, Osaka, 567-0047, Japan*

[2]*KEK Theory Center, Institute of Particle and Nuclear Studies, High Energy Accelerator Research Organization, 1-1, Oho, Ibaraki, 305-0801, Japan*

[3]*Nishogakusha University, 6-16, Sanbancho, Chiyoda, Tokyo, 102-8336, Japan*

(Received 26 November 2011; revised manuscript received 24 April 2012; published 5 July 2012)

We study heavy hadron spectroscopy near open bottom thresholds. We employ B and B^* mesons as effective degrees of freedom near the thresholds, and consider meson exchange potentials between them. All possible composite states which can be constructed from the B and B^* mesons are studied up to the total angular momentum $J \leq 2$. We consider, as exotic states, isosinglet states with exotic J^{PC} quantum numbers and isotriplet states. We solve numerically the Schrödinger equation with channel couplings for each state. The masses of twin resonances $Z_b(10\,610)$ and $Z_b(10\,650)$ recently found by Belle are reproduced. We predict several possible bound and/or resonant states in other channels for future experiments.

DOI: 10.1103/PhysRevD.86.014004 PACS numbers: 12.39.Jh, 12.39.Hg, 13.30.Eg, 14.20.−c

I. INTRODUCTION

Exotic hadrons are studied extensively in recent hadron physics. There have been many analyses which imply that they are multiquark systems or hadronic molecules. In strangeness sector, there are several candidates of exotic hadrons, such as $f_0(980)$, $a_0(980)$, $\Lambda(1405)$, and so on. The scalar mesons $f_0(980)$ and $a_0(980)$ may be regarded as tetraquark systems or $K\bar{K}$ molecules [1,2]. $\Lambda(1405)$ is considered to be generated dynamically by $\bar{K}N$ and $\pi\Sigma$ [3]. In charm and bottom sectors, recently many candidates of exotic hadrons have been reported in experiments and also actively discussed in theoretical studies [4–8]. $D_s(2317)$ and $D_s(2460)$ may be tetraquarks or KD molecules. X(3872), Y(4260), $Z(4050)^{\pm}$, $Z(4250)^{\pm}$, $Z(4430)^{\pm}$, and so on are also candidates of exotics states. Especially $Z(4050)^{\pm}$, $Z(4250)^{\pm}$, and $Z(4430)^{\pm}$ cannot be simple charmonia ($c\bar{c}$) because they are electrically charged. There are also exotic hadrons in bottom flavors. Y_b is the first candidate of exotic bottom hadrons. More recently, $Z_b(10\,610)^{\pm}$ and $Z_b(10\,650)^{\pm}$ with isospin one have been reported by Belle [9,10]. The reported masses and widths of the two resonances are $M(Z_b(10\,610)) = 10\,607.2 \pm 2.0$ MeV, $\Gamma(Z_b(10\,610)) = 18.4 \pm 2.4$ MeV and $M(Z_b(10\,650)) = 10\,652.2 \pm 1.5$ MeV, $\Gamma(Z_b(10\,650)) = 11.5 \pm 2.2$ MeV. They also cannot be simple bottomonia ($b\bar{b}$) because they are electrically charged.

Well below the thresholds in the heavy quark systems, quarkonia are described by heavy quark degrees of freedom, Q and $\bar{Q}$ (Q = b, c). Above the thresholds, however, it is a nontrivial problem whether the resonant states are still explained by the quarkonium picture. Clearly, a pair of heavy quark and antiquark ($Q\bar{Q}$) are not sufficient effective degrees of freedom to form the resonances, because they are affected by the scattering states of the two open heavy mesons. Indeed, many resonant states are found around the thresholds in experiments. However, they do not fit into the ordinary classification scheme of hadrons, such as the quark model calculation. Properties for masses, decay widths, branching ratios, and so forth, are not predicted by the simple quarkonium picture [4]. Therefore, it is necessary to introduce components other than $Q\bar{Q}$ as effective degrees of freedom around the thresholds.

Instead of the dynamics of $Q\bar{Q}$, in the present paper, we study the dynamics described by a pair of a pseudoscalar meson $P \sim (\bar{Q}q)_{\rm spin0}$ or a vector meson $P^* \sim (\bar{Q}q)_{\rm spin1}$ (q = u, d) and their antimesons $\bar{P}$ or $\bar{P}^*$, which are relevant hadronic degrees of freedom around the thresholds. In the following, we introduce the notation $P^{(*)}$ for P or P^* for simplicity. We discuss the possible existence of the $P^{(*)}\bar{P}^{(*)}$ bound and/or resonant states near the thresholds. An interesting feature is that the pseudoscalar P meson and the vector P^* meson become degenerate in mass in the heavy quark limit ($M_Q \to \infty$). The mass degeneracy originates from the suppression of the Pauli term in the magnetic gluon sector in QCD, which is the quantity of order $\mathcal{O}(1/M_Q)$ with heavy quark mass M_Q [11,12]. Therefore, the effective degrees of freedom at the threshold are given, not only by $P\bar{P}$, but also by combinations, such as $P^*\bar{P}$, $P\bar{P}^*$, and $P^*\bar{P}^*$. Because $P^{(*)}$ includes a heavy antiquark $\bar{Q}$ and a light quark q, the Lagrangian of P and P^* meson systems is given with respecting the heavy quark symmetry (spin symmetry) and chiral symmetry [12–21].

A new degree of freedom which does not exist in the $Q\bar{Q}$ systems but does only in the $P^{(*)}\bar{P}^{(*)}$ systems is an isospin. Then, there appears one-pion-exchange potential (OPEP) between $P^{(*)}$ and $\bar{P}^{(*)}$ mesons at long distances of order $1/m_\pi$ with pion mass m_π. What is interesting in the OPEP between $P^{(*)}$ and $\bar{P}^{(*)}$ is that it causes a mixing between states of different angular momentum, such as L and $L \pm 2$, through its tensor component. Therefore, it is expected that the $P^{(*)}\bar{P}^{(*)}$ systems behave differently from the quarkonium systems. In reality, in addition to the one pion exchange dominated at long distances, there are multiple pion ($\pi\pi$, $\pi\pi\pi$, etc.) exchange, heavy meson (ρ, ω, σ, etc.) exchange at short distances as well. With these potentials, we solve the two-body Schrödinger equation with channel couplings and discuss the existence of bound and/or resonant states of $\mathrm{P}^{(*)}\bar{\mathrm{P}}^{(*)}$.

In this paper, we study $\mathrm{P}^{(*)}\bar{\mathrm{P}}^{(*)}$ systems, with exotic quantum numbers which cannot be accessed by quarkonia. The first group is for isosinglet states with $I = 0$. We recall that the possible J^{PC} of quarkonia are $J^{PC} = 0^{-+}$ (η_b), 0^{++} ($\chi_{\mathrm{b}0}$) for $J = 0$, J^{--} (Υ), J^{+-} ($\mathrm{h_b}$), J^{++} ($\chi_{\mathrm{b}1}$) for odd $J \geq 1$, and J^{--}, J^{-+}, J^{++} ($\chi_{\mathrm{b}2}$) for even $J \geq 2$, where examples of bottomonia are shown in the parentheses. However, there cannot be $J^{PC} = 0^{--}$ and 0^{+-}, J^{-+} with odd $J \geq 1$, and J^{+-} with even $J \geq 2$ in the quarkonia. These quantum numbers are called exotic J^{PC}, and it has been discussed that they are the signals for exotics including the $\mathrm{P}^{(*)}\bar{\mathrm{P}}^{(*)}$ systems and glueballs. The second group is for isospin triplet states with $I = 1$. It is obvious that the quarkonia themselves cannot be isotriplet. To have a finite isospin, there must be additional light quark degrees of freedom [22]. In this regard, $\mathrm{P}^{(*)}$ and $\bar{\mathrm{P}}^{(*)}$ mesons have isospin half, and therefore the $\mathrm{P}^{(*)}\bar{\mathrm{P}}^{(*)}$ composite systems can be isospin triplet. We observe that, near the thresholds, the $\mathrm{P}^{(*)}\bar{\mathrm{P}}^{(*)}$ systems can access to more variety of quantum numbers than the $\mathrm{Q}\bar{\mathrm{Q}}$ systems. In this paper, we focus on the bottom sector ($\mathrm{P} = \mathrm{B}$ and $\mathrm{P}^* = \mathrm{B}^*$), because the heavy quark symmetry works better than the charm sector.

In the previous works, Ericson and Karl estimated the OPEP in hadronic molecules within strangeness sector and indicated the importance of tensor interaction in this system [23]. Törnqvist analyzed one pion exchange force between two mesons for many possible quantum numbers in [24,25]. Inspired by the discovery of X(3872), the hadronic molecular model has been developed by many authors [6,8,26–30]. For $\mathrm{Z_b}$'s, many works have already been done since the Belle's discovery. As candidates of exotic states, molecular structure has been studied [31–37], and also tetraquark structure [38–43]. The existence of $\mathrm{Z_b}$'s has also been investigated in the decays of $\Upsilon(5S)$ [44–47]. Our study based on the molecular picture of $\mathrm{P}^{(*)}\bar{\mathrm{P}}^{(*)}$ differs from the previous works in that we completely take into account the degeneracy of pseudoscalar meson B and a vector meson B^* due to the heavy quark symmetry, and fully consider channel couplings of $\mathrm{B}^{(*)}$ and $\bar{\mathrm{B}}^{(*)}$. In the previous publications, the low-lying molecular states around $\mathrm{Z_b}$'s which can be produced from the decay of $\Upsilon(5S)$ were studied systematically and qualitatively [48,49]. Our present work covers them also.

This paper is organized as follows. In Sec. II, we introduce (i) the π exchange potential and (ii) the $\pi\rho\omega$ potential between $\mathrm{B}^{(*)}$ and $\bar{\mathrm{B}}^{(*)}$ mesons. To obtain the potentials, we respect the heavy quark symmetry for the $\mathrm{B}^{(*)}\mathrm{B}^{(*)}\pi$, $\mathrm{B}^{(*)}\mathrm{B}^{(*)}\rho$ and $\mathrm{B}^{(*)}\mathrm{B}^{(*)}\omega$ vertices. In Sec. III, we classify all the possible states composed by a pair of $\mathrm{B}^{(*)}$ and $\bar{\mathrm{B}}^{(*)}$ mesons with exotic quantum numbers $I^G(J^{PC})$ with isospin I, G parity, total angular momentum J, parity P, and charge conjugation C. (C in $I = 1$ is defined only for states of $I_z = 0$.) In Sec. IV, we solve numerically the Schrödinger equations with channel couplings and discuss the bound and/or resonant states of the $\mathrm{B}^{(*)}\bar{\mathrm{B}}^{(*)}$ systems. We employ the hadronic molecular picture and only consider the $\mathrm{B}^{(*)}\bar{\mathrm{B}}^{(*)}$ states. In practice, there are bottomonium and light meson states which couple to these states. The effect of these couplings as quantum corrections is estimated in Sec. V. In Sec. VI, we discuss the possible decay modes of these states. Section VII is devoted to summary.

II. INTERACTIONS WITH HEAVY QUARK SYMMETRY

$\mathrm{B}^{(*)}$ mesons have a heavy antiquark $\bar{\mathrm{b}}$ and a light quark $\mathrm{q} = \mathrm{u}, \mathrm{d}$. The dynamics of the $\mathrm{B}^{(*)}\bar{\mathrm{B}}^{(*)}$ systems is given by the two symmetries: the heavy quark symmetry for heavy quarks and chiral symmetry for light quarks. These two symmetries provide the vertices of π meson and of vector meson ($v = \rho, \omega$) with open heavy flavor (bottom) mesons P and P^* (P for B and P^* for B^*)

$$\mathcal{L}_{\pi HH} = g\,\mathrm{tr}\bar{H}_a H_b \gamma_\nu \gamma_5 A^\nu_{ba}, \tag{1}$$

$$\mathcal{L}_{vHH} = -i\beta\,\mathrm{tr}\bar{H}_a H_b v^\mu (\rho_\mu)_{ba} + i\lambda\,\mathrm{tr}\bar{H}_a H_b \sigma_{\mu\nu} F_{\mu\nu}(\rho)_{ba}, \tag{2}$$

where the multiplet field H containing P and P^* is defined by

$$H_a = \frac{1+\not{v}}{2}[P^*_{a\mu}\gamma^\mu - P_a\gamma_5], \tag{3}$$

with the four-velocity v_μ of the heavy mesons [11]. The conjugate field is defined by $\bar{H}_a = \gamma_0 H_a^\dagger \gamma_0$, and the index a denotes up and down flavors. The axial current is given by $A_\mu \simeq \frac{i}{f_\pi}\partial_\mu \hat{\pi}$ with

$$\hat{\pi} = \begin{pmatrix} \frac{\pi^0}{\sqrt{2}} & \pi^+ \\ \pi^- & -\frac{\pi^0}{\sqrt{2}} \end{pmatrix}, \tag{4}$$

where $f_\pi = 135$ MeV is the pion decay constant. The coupling constant $|g| = 0.59$ for πPP^* is determined with reference to the observed decay width $\Gamma = 96$ keV for $\mathrm{D}^* \to \mathrm{D}\pi$ [50], assuming that the charm quark is sufficiently heavy. The coupling constant g for $\pi\mathrm{BB}^*$ would be different from the one for $\pi\mathrm{DD}^*$ because of $1/m_\mathrm{Q}$ corrections with the heavy quark mass m_Q [51]. However, the lattice simulation in the heavy quark limit suggests a similar value as adopted above [52], allowing us to use the common value for D and B. The coupling of $\pi P^* P^*$, which is difficult to access from experiments, is also fixed thanks to the heavy quark symmetry. Note that the coupling of πPP does not exist due to the parity conservation. The coupling constants β and λ are determined by the radiative decays of D^* meson and semileptonic decays of B meson with vector meson dominance as $\beta = 0.9$ and $\lambda = 0.56\ \mathrm{GeV}^{-1}$ by following

Ref. [53]. The vector (ρ and ω) meson field is defined by

$$\rho_\mu = i\frac{g_V}{\sqrt{2}}\hat{\rho}_\mu, \tag{5}$$

with

$$\hat{\rho}_\mu = \begin{pmatrix} \frac{\rho^0}{\sqrt{2}} + \frac{\omega}{\sqrt{2}} & \rho^+ \\ \rho^- & -\frac{\rho^0}{\sqrt{2}} + \frac{\omega}{\sqrt{2}} \end{pmatrix}_\mu, \tag{6}$$

and its field tensor by

$$F_{\mu\nu}(\rho) = \partial_\mu\rho_\nu - \partial_\nu\rho_\mu + [\rho_\mu, \rho_\nu], \tag{7}$$

where $g_V = 5.8$ is the coupling constant for $\rho \to \pi\pi$ decay.

From Eq. (1), we obtain the πPP^* and πP^*P^* vertices

$$\mathcal{L}_{\pi PP^*} = 2\frac{g}{f_\pi}(P_a^\dagger P_{b\mu}^* + P_{a\mu}^{*\dagger}P_b)\partial^\mu\hat{\pi}_{ab}, \tag{8}$$

$$\mathcal{L}_{\pi P^*P^*} = 2i\frac{g}{f_\pi}\epsilon^{\alpha\beta\mu\nu}v_\alpha P_{a\beta}^{*\dagger}P_{b\mu}^*\partial_\nu\hat{\pi}_{ab}. \tag{9}$$

The $\pi\bar{P}\bar{P}^*$ and $\pi\bar{P}^*\bar{P}^*$ vertices are obtained by changing the sign of the πPP^* and πP^*P^* vertices in Eqs. (8) and (9). Similarly, from Eq. (2) we derive the vPP, vPP^*, and vP^*P^* vertices ($v = \rho, \omega$) as

$$\mathcal{L}_{vPP} = -\sqrt{2}\beta g_V P_b P_a^\dagger v\cdot\hat{\rho}_{ba}, \tag{10}$$

$$\mathcal{L}_{vPP^*} = -2\sqrt{2}\lambda g_V v_\mu\epsilon^{\mu\nu\alpha\beta}(P_a^\dagger P_{b\beta}^* - P_{a\beta}^{*\dagger}P_b)\partial_\nu(\hat{\rho}_\alpha)_{ba}, \tag{11}$$

$$\begin{aligned}\mathcal{L}_{vP^*P^*} = {}& \sqrt{2}\beta g_V P_b^* P_a^{*\dagger} v\cdot\hat{\rho}_{ba} \\ &+ i2\sqrt{2}\lambda g_V P_{a\mu}^{*\dagger}P_{b\nu}^*(\partial^\mu(\hat{\rho}^\nu)_{ba} - \partial^\nu(\hat{\rho}^\mu)_{ba}).\end{aligned} \tag{12}$$

Because of the G parity, the signs of vertices for $v\bar{P}\bar{P}$, $v\bar{P}\bar{P}^*$, and $v\bar{P}^*\bar{P}^*$ are opposite to those of vPP, vPP^*, and vP^*P^*, respectively, for $v = \omega$, while they are the same for $v = \rho$.

It is important that the scatterings $P^{(*)}\bar{P}^{(*)} \to P^{(*)}\bar{P}^{(*)}$ include not only diagonal components $P\bar{P}^* \to P^*\bar{P}$ and $P^*\bar{P}^* \to P^*\bar{P}^*$ but also off-diagonal components $P\bar{P} \to P^*\bar{P}^*$ and $P\bar{P}^* \to P^*\bar{P}^*$. The OPEPs for $P\bar{P}^* \to P^*\bar{P}$ and $P^*\bar{P}^* \to P^*\bar{P}^*$ are given from the vertices (8) and (9) in the heavy quark limit as

$$\begin{aligned}V^\pi_{P_1\bar{P}_2^*\to P_1^*\bar{P}_2} = {}& -\left(\sqrt{2}\frac{g}{f_\pi}\right)^2\frac{1}{3}[\vec{\varepsilon}_1^*\cdot\vec{\varepsilon}_2 C(r;m_\pi) \\ &+ S_{\varepsilon_1^*,\varepsilon_2}T(r;m_\pi)]\vec{\tau}_1\cdot\vec{\tau}_2,\end{aligned} \tag{13}$$

$$\begin{aligned}V^\pi_{P_1^*\bar{P}_2^*\to P_1^*\bar{P}_2^*} = {}& -\left(\sqrt{2}\frac{g}{f_\pi}\right)^2\frac{1}{3}[\vec{T}_1\cdot\vec{T}_2 C(r;m_\pi) \\ &+ S_{T_1,T_2}T(r;m_\pi)]\vec{\tau}_1\cdot\vec{\tau}_2,\end{aligned} \tag{14}$$

and the OPEPs for $P\bar{P} \to P^*\bar{P}^*$ and $P\bar{P}^* \to P^*\bar{P}^*$ are given as

$$\begin{aligned}V^\pi_{P_1\bar{P}_2\to P_1^*\bar{P}_2^*} = {}& -\left(\sqrt{2}\frac{g}{f_\pi}\right)^2\frac{1}{3}[\vec{\varepsilon}_1^*\cdot\vec{\varepsilon}_2^* C(r;m_\pi) \\ &+ S_{\varepsilon_1^*,\varepsilon_2^*}T(r;m_\pi)]\vec{\tau}_1\cdot\vec{\tau}_2,\end{aligned} \tag{15}$$

$$\begin{aligned}V^\pi_{P_1\bar{P}_2^*\to P_1^*\bar{P}_2^*} = {}& \left(\sqrt{2}\frac{g}{f_\pi}\right)^2\frac{1}{3}[\vec{\varepsilon}_1^*\cdot\vec{T}_2 C(r;m_\pi) \\ &+ S_{\varepsilon_1^*,T_2}T(r;m_\pi)]\vec{\tau}_1\cdot\vec{\tau}_2.\end{aligned} \tag{16}$$

Here, three polarizations are possible for P^* as defined by $\vec{\varepsilon}^{(\pm)} = (\mp1/\sqrt{2}, -i/\sqrt{2}, 0)$ and $\vec{\varepsilon}^{(0)} = (0,0,1)$, and the spin-one operator $\vec{T}$ is defined by $T^i_{\lambda'\lambda} = i\varepsilon^{ijk}\varepsilon_j^{(\lambda')\dagger}\varepsilon_k^{(\lambda)}$. As a convention, we assign $\vec{\varepsilon}^{(\lambda)}$ for an incoming vector particle and $\vec{\varepsilon}^{(\lambda)*}$ for an outgoing vector particle. Here, $\vec{\tau}_1$ and $\vec{\tau}_2$ are isospin operators for $P_1^{(*)}$ and $\bar{P}_2^{(*)}$. We define the tensor operators

$$S_{\varepsilon_1^*,\varepsilon_2} = 3(\vec{\varepsilon}^{(\lambda_1)*}\cdot\hat{r})(\vec{\varepsilon}^{(\lambda_2)}\cdot\hat{r}) - \vec{\varepsilon}^{(\lambda_1)*}\cdot\vec{\varepsilon}^{(\lambda_2)}, \tag{17}$$

$$S_{T_1,T_2} = 3(\vec{T}_1\cdot\hat{r})(\vec{T}_2\cdot\hat{r}) - \vec{T}_1\cdot\vec{T}_2, \tag{18}$$

$$S_{\varepsilon_1^*,\varepsilon_2^*} = 3(\vec{\varepsilon}^{(\lambda_1)*}\cdot\hat{r})(\vec{\varepsilon}^{(\lambda_2)*}\cdot\hat{r}) - \vec{\varepsilon}^{(\lambda_1)*}\cdot\vec{\varepsilon}^{(\lambda_2)*}, \tag{19}$$

$$S_{\varepsilon_1^*,T_2} = 3(\vec{\varepsilon}^{(\lambda_1)*}\cdot\hat{r})(\vec{T}_2\cdot\hat{r}) - \vec{\varepsilon}^{(\lambda_1)*}\cdot\vec{T}_2. \tag{20}$$

The ρ meson exchange potentials are derived by using the same notation of the OPEPs and the vertices in Eqs. (10)–(12),

$$V^v_{P_1\bar{P}_2\to P_1\bar{P}_2} = \left(\frac{\beta g_V}{2m_v}\right)^2\frac{1}{3}C(r;m_v)\vec{\tau}_1\cdot\vec{\tau}_2, \tag{21}$$

$$V^v_{P_1\bar{P}_2^*\to P_1\bar{P}_2^*} = \left(\frac{\beta g_V}{2m_v}\right)^2\frac{1}{3}C(r;m_v)\vec{\tau}_1\cdot\vec{\tau}_2, \tag{22}$$

$$\begin{aligned}V^v_{P_1\bar{P}_2^*\to P_1^*\bar{P}_2} = {}& (2\lambda g_V)^2\frac{1}{3}[2\vec{\varepsilon}_1^*\cdot\vec{\varepsilon}_2 C(r;m_v) \\ &- S_{\varepsilon_1^*,\varepsilon_2}T(r;m_v)]\vec{\tau}_1\cdot\vec{\tau}_2,\end{aligned} \tag{23}$$

$$\begin{aligned}V^v_{P_1^*\bar{P}_2^*\to P_1^*\bar{P}_2^*} = {}& (2\lambda g_V)^2\frac{1}{3}[2\vec{T}_1\cdot\vec{T}_2 C(r;m_v) \\ &- S_{T_1,T_2}T(r;m_v)]\vec{\tau}_1\cdot\vec{\tau}_2 \\ &+ \left(\frac{\beta g_V}{2m_v}\right)^2\frac{1}{3}C(r;m_v)\vec{\tau}_1\cdot\vec{\tau}_2,\end{aligned} \tag{24}$$

$$\begin{aligned}V^v_{P_1\bar{P}_2\to P_1^*\bar{P}_2^*} = {}& (2\lambda g_V)^2\frac{1}{3}[2\vec{\varepsilon}_1^*\cdot\vec{\varepsilon}_2^* C(r;m_v) \\ &- S_{\varepsilon_1^*,\varepsilon_2^*}T(r;m_v)]\vec{\tau}_1\cdot\vec{\tau}_2,\end{aligned} \tag{25}$$

$$\begin{aligned}V^v_{P_1\bar{P}_2^*\to P_1^*\bar{P}_2^*} = {}& -(2\lambda g_V)^2\frac{1}{3}[2\vec{\varepsilon}_1^*\cdot\vec{T}_2 C(r;m_v) \\ &- S_{\varepsilon_1^*,T_2}T(r;m_v)]\vec{\tau}_1\cdot\vec{\tau}_2,\end{aligned} \tag{26}$$

for $v = \rho$. The ω exchange potentials are obtained by changing the overall sign from the above equations with $v = \omega$ and by removing the isospin factor $\vec{\tau}_1\cdot\vec{\tau}_2$.

To estimate the size effect of mesons, we introduce a form factor $(\Lambda^2 - m_h^2)/(\Lambda^2 + \vec{q}^2)$ in the momentum space at vertices of hPP, hPP^*, and hP^*P^* ($h = \pi$, ρ, and ω). Here, $\vec{q}$ and m_h are momentum and mass of the exchanged meson, and Λ is the cutoff parameter. Then, $C(r; m_h)$ and $T(r; m_h)$ are defined as

$$C(r; m_h) = \int \frac{d^3\vec{q}}{(2\pi)^3} \frac{m_h^2}{\vec{q}^2 + m_h^2} e^{i\vec{q}\cdot\vec{r}} F(\vec{q}; m_h), \tag{27}$$

$$T(r; m_h) S_{12}(\hat{r}) = \int \frac{d^3\vec{q}}{(2\pi)^3} \frac{-\vec{q}^2}{\vec{q}^2 + m_h^2} S_{12}(\hat{q}) e^{i\vec{q}\cdot\vec{r}} F(\vec{q}; m_h), \tag{28}$$

with $S_{12}(\hat{x}) = 3(\vec{\sigma}_1 \cdot \hat{x})(\vec{\sigma}_2 \cdot \hat{x}) - \vec{\sigma}_1 \cdot \vec{\sigma}_2$, and $F(\vec{q}; m_h) = (\Lambda^2 - m_h^2)^2/(\Lambda^2 + \vec{q}^2)^2$. The cutoff Λ is determined from the size of $\mathrm{B}^{(*)}$ based on the quark model as discussed in Refs. [54,55]. There, the cutoff parameter is $\Lambda = 1070$ MeV when the π exchange potential is employed, while $\Lambda = 1091$ MeV when the $\pi\rho\omega$ potential is employed.

As a brief summary, we emphasize again that, according to the heavy quark symmetry, not only the $\mathrm{B}\bar{\mathrm{B}}^* \to \mathrm{B}^*\bar{\mathrm{B}}$ and $\mathrm{B}^*\bar{\mathrm{B}}^* \to \mathrm{B}^*\bar{\mathrm{B}}^*$ transitions but also the $\mathrm{B}\bar{\mathrm{B}} \to \mathrm{B}^*\bar{\mathrm{B}}^*$ and $\mathrm{B}\bar{\mathrm{B}}^* \to \mathrm{B}^*\bar{\mathrm{B}}^*$ transitions become important as channel couplings. In the next section, we will see that the latter two transitions supply the strong tensor force, through the channel mixing B and B^* as well as different angular momentum, such as L and $L \pm 2$.

III. CLASSIFICATION OF THE $\mathrm{B}^{(*)}\bar{\mathrm{B}}^{(*)}$ STATES

We classify all the possible quantum numbers $I^G(J^{PC})$ with isospin I, G parity, total angular momentum J, parity P, and charge conjugation C for the states which can be composed by a pair of $\mathrm{B}^{(*)}$ and $\bar{\mathrm{B}}^{(*)}$ mesons. The charge conjugation C is defined for $I = 0$ or $I_z = 0$ components for $I = 1$, and is related to the G parity by $G = (-1)^I C$. In the present discussion, we restrict upper limit of the total angular momentum as $J \le 2$, because too higher angular momentum will be disfavored to form bound or resonant states. The $\mathrm{B}^{(*)}\bar{\mathrm{B}}^{(*)}$ components in the wave functions for various J^{PC} are listed in Table I. We use the notation $^{2S+1}L_J$ to denote the total spin S and relative angular momentum L of the two-body states of $\mathrm{B}^{(*)}$ and $\bar{\mathrm{B}}^{(*)}$ mesons. We note that there are not only $\mathrm{B}\bar{\mathrm{B}}$ and $\mathrm{B}^*\bar{\mathrm{B}}^*$ components but also $\mathrm{B}\bar{\mathrm{B}}^* \pm \bar{\mathrm{B}}\mathrm{B}^*$ components. The $J^{PC} = 0^{+-}$ state cannot be generated by a combination of $\mathrm{B}^{(*)}$ and $\bar{\mathrm{B}}^{(*)}$ mesons [56]. For $I = 0$, there are many $\mathrm{B}^{(*)}\bar{\mathrm{B}}^{(*)}$ states whose quantum number J^{PC} are the same as those of the quarkonia as shown in the third row of $I = 0$. In the present study, however, we do not consider these states, because we have not yet included mixing terms between the quarkonia and the $\mathrm{B}^{(*)}\bar{\mathrm{B}}^{(*)}$ states. This problem will be left as future works. Therefore, for $I = 0$, we consider only the exotic quantum numbers $J^{PC} = 0^{--}$, 1^{-+}, and 2^{+-}. The states of $I = 1$ are clearly not accessible by quarkonia. We investigate all possible J^{PC} states listed in Table I.

From Eqs. (13)–(16) and (21)–(26), we obtain the potentials with channel couplings for each quantum number $I^G(J^{PC})$. For each state, the Hamiltonian is given as a sum of the kinetic energy and the potential with channel couplings in a form of a matrix. Breaking of the heavy quark symmetry is taken into account by mass difference between B and B^* mesons in the kinetic term. The explicit forms of the Hamiltonian for each $I^G(J^{PC})$ are presented in Appendix A. For example, the $J^{PC} = 1^{+-}$ state has four components, $\frac{1}{\sqrt{2}}(\mathrm{B}\bar{\mathrm{B}}^* - \mathrm{B}^*\bar{\mathrm{B}})(^3S_1)$, $\frac{1}{\sqrt{2}} \times (\mathrm{B}\bar{\mathrm{B}}^* - \mathrm{B}^*\bar{\mathrm{B}})(^3D_1)$, $\mathrm{B}^*\bar{\mathrm{B}}^*(^3S_1)$, $\mathrm{B}^*\bar{\mathrm{B}}^*(^3D_1)$ and hence it gives a potential in the form of 4×4 matrix as Eqs. (A6), (A17), and (A28).

TABLE I. Various components of the $\mathrm{B}^{(*)}\bar{\mathrm{B}}^{(*)}$ states for several J^{PC} ($J \le 2$). The exotic quantum numbers which cannot be assigned to bottomonia $\mathrm{b}\bar{\mathrm{b}}$ are indicated by $\surd$. The 0^{+-} state cannot be neither bottomonium nor $\mathrm{B}^{(*)}\bar{\mathrm{B}}^{(*)}$ states.

J^{PC}	Components	Exoticness	
		$I = 0$	$I = 1$
0^{+-}	$\cdots$	$\surd$	$\surd$
0^{++}	$\mathrm{B}\bar{\mathrm{B}}(^1S_0)$, $\mathrm{B}^*\bar{\mathrm{B}}^*(^1S_0)$, $\mathrm{B}^*\bar{\mathrm{B}}^*(^5D_0)$	$\chi_{\mathrm{b}0}$	$\surd$
0^{--}	$\frac{1}{\sqrt{2}}(\mathrm{B}\bar{\mathrm{B}}^* + \mathrm{B}^*\bar{\mathrm{B}})(^3P_0)$	$\surd$	$\surd$
0^{-+}	$\frac{1}{\sqrt{2}}(\mathrm{B}\bar{\mathrm{B}}^* - \mathrm{B}^*\bar{\mathrm{B}})(^3P_0)$, $\mathrm{B}^*\bar{\mathrm{B}}^*(^3P_0)$	η_{b}	$\surd$
1^{+-}	$\frac{1}{\sqrt{2}}(\mathrm{B}\bar{\mathrm{B}}^* - \mathrm{B}^*\bar{\mathrm{B}})(^3S_1)$, $\frac{1}{\sqrt{2}}(\mathrm{B}\bar{\mathrm{B}}^* - \mathrm{B}^*\bar{\mathrm{B}})(^3D_1)$, $\mathrm{B}^*\bar{\mathrm{B}}^*(^3S_1)$, $\mathrm{B}^*\bar{\mathrm{B}}^*(^3D_1)$	h_{b}	$\surd$
1^{++}	$\frac{1}{\sqrt{2}}(\mathrm{B}\bar{\mathrm{B}}^* + \mathrm{B}^*\bar{\mathrm{B}})(^3S_1)$, $\frac{1}{\sqrt{2}}(\mathrm{B}\bar{\mathrm{B}}^* + \mathrm{B}^*\bar{\mathrm{B}})(^3D_1)$, $\mathrm{B}^*\bar{\mathrm{B}}^*(^5D_1)$	$\chi_{\mathrm{b}1}$	$\surd$
1^{--}	$\mathrm{B}\bar{\mathrm{B}}(^1P_1)$, $\frac{1}{\sqrt{2}}(\mathrm{B}\bar{\mathrm{B}}^* + \mathrm{B}^*\bar{\mathrm{B}})(^3P_1)$, $\mathrm{B}^*\bar{\mathrm{B}}^*(^1P_1)$, $\mathrm{B}^*\bar{\mathrm{B}}^*(^5P_1)$, $\mathrm{B}^*\bar{\mathrm{B}}^*(^5F_1)$	Υ	$\surd$
1^{-+}	$\frac{1}{\sqrt{2}}(\mathrm{B}\bar{\mathrm{B}}^* - \mathrm{B}^*\bar{\mathrm{B}})(^3P_1)$, $\mathrm{B}^*\bar{\mathrm{B}}^*(^3P_1)$	$\surd$	$\surd$
2^{+-}	$\frac{1}{\sqrt{2}}(\mathrm{B}\bar{\mathrm{B}}^* - \mathrm{B}^*\bar{\mathrm{B}})(^3D_2)$, $\mathrm{B}^*\bar{\mathrm{B}}^*(^3D_2)$	$\surd$	$\surd$
2^{++}	$\mathrm{B}\bar{\mathrm{B}}(^1D_2)$, $\frac{1}{\sqrt{2}}(\mathrm{B}\bar{\mathrm{B}}^* + \mathrm{B}^*\bar{\mathrm{B}})(^3D_2)$, $\mathrm{B}^*\bar{\mathrm{B}}^*(^1D_2)$, $\mathrm{B}^*\bar{\mathrm{B}}^*(^5S_2)$, $\mathrm{B}^*\bar{\mathrm{B}}^*(^5D_2)$, $\mathrm{B}^*\bar{\mathrm{B}}^*(^5G_2)$	$\chi_{\mathrm{b}2}$	$\surd$
2^{-+}	$\frac{1}{\sqrt{2}}(\mathrm{B}\bar{\mathrm{B}}^* - \mathrm{B}^*\bar{\mathrm{B}})(^3P_2)$, $\frac{1}{\sqrt{2}}(\mathrm{B}\bar{\mathrm{B}}^* - \mathrm{B}^*\bar{\mathrm{B}})(^3F_2)$, $\mathrm{B}^*\bar{\mathrm{B}}^*(^3P_2)$, $\mathrm{B}^*\bar{\mathrm{B}}^*(^3F_2)$	$\eta_{\mathrm{b}2}$	$\surd$
2^{--}	$\frac{1}{\sqrt{2}}(\mathrm{B}\bar{\mathrm{B}}^* + \mathrm{B}^*\bar{\mathrm{B}})(^3P_2)$, $\frac{1}{\sqrt{2}}(\mathrm{B}\bar{\mathrm{B}}^* + \mathrm{B}^*\bar{\mathrm{B}})(^3F_2)$, $\mathrm{B}^*\bar{\mathrm{B}}^*(^5P_2)$, $\mathrm{B}^*\bar{\mathrm{B}}^*(^5F_2)$	$\psi_{\mathrm{b}2}$	$\surd$

IV. NUMERICAL RESULTS

To obtain the solutions of the $\mathrm{B}^{(*)}\bar{\mathrm{B}}^{(*)}$ states, we solve numerically the Schrödinger equations which are second-order differential equations with channel couplings. As numerics, the renormalized Numerov method developed in Ref. [57] is adopted. The resonant states are found from the phase shift δ as a function of the scattering energy E. The resonance position E_r is defined by an inflection point of the phase shift $\delta(E)$ and the resonance width by $\Gamma_r = 2/(d\delta/dE)_{E=E_r}$ following Ref. [58]. To check consistency of our method with others, we also use the complex scaling method [59]. We obtain an agreement in results between the renormalized Nemerov method and the complex scaling method.

In Table II, we summarize the result of the obtained bound and resonant states, and their possible decay modes to quarkonium and light flavor meson. For decay modes, the ρ meson can be either real or virtual depending on the mass of the decaying particle, depending on the resonance energy which is either sufficient or not to emit the real state of ρ or ω meson. $\rho^*(\omega^*)$ indicates that it is a virtual state in radiative decays assuming the vector meson dominance. We show the mass spectrum of these states in Fig. 1.

Let us see the states of isospin $I = 1$. Interestingly, having the present potential we find the twin states in the $I^G(J^{PC}) = 1^+(1^{+-})$ near the $\mathrm{B}\bar{\mathrm{B}}^*$ and $\mathrm{B}^*\bar{\mathrm{B}}^*$ thresholds; a bound state slightly below the $\mathrm{B}\bar{\mathrm{B}}^*$ threshold, and a resonant state slightly above the $\mathrm{B}^*\bar{\mathrm{B}}^*$ threshold. The binding energy is 8.5 MeV, and the resonance energy and decay width are 50.4 MeV and 15.1 MeV, respectively, from the $\mathrm{B}\bar{\mathrm{B}}^*$ threshold. The twin states are obtained when the $\pi\rho\omega$ potential is used. We interpret them as the $\mathrm{Z}_\mathrm{b}(10\,610)$ and $\mathrm{Z}_\mathrm{b}(10\,650)$ observed in the Belle experiment [9,10]. It should be emphasized that the interaction in the present study has been determined in the previous works without knowing the experimental data of Z_b's [54,55].

Several comments are in order. First, the bound state of lower energy has been obtained in the coupled channel method of $\mathrm{B}\bar{\mathrm{B}}^*$ and $\mathrm{B}^*\bar{\mathrm{B}}^*$ channels. In reality, however, they also couple to other lower channels such as πh_b, $\pi\Upsilon$ and so on as shown in Table I. Once these decay channels are included, the bound state will be a resonant state with a finite width. A qualitative discussion will be given in Sec. V. Second, when the π exchange potential is used, only the lower bound state is obtained but the resonant state is not. However, we have verified that a small change in the π exchange potential generates, as well as the bound state, the corresponding resonant state also. Therefore, the pion dominance is working for the $\mathrm{B}\bar{\mathrm{B}}^*$ and $\mathrm{B}^*\bar{\mathrm{B}}^*$ systems. (See also the discussion in Appendix B.) Third, it would provide a direct evidence of these states to be $\mathrm{B}\bar{\mathrm{B}}^*$ and $\mathrm{B}^*\bar{\mathrm{B}}^*$ molecules if the $\mathrm{B}\bar{\mathrm{B}}^*$ and $\mathrm{B}^*\bar{\mathrm{B}}^*$ decays are observed in experiments. Whether the energies are below or above the thresholds is also checked by the observation of these decays.

In other channels, we further predict the $\mathrm{B}^{(*)}\bar{\mathrm{B}}^{(*)}$ bound and resonant states. The $I^G(J^{PC}) = 1^-(0^{++})$ state is a bound state with binding energy 6.5 MeV from the $\mathrm{B}\bar{\mathrm{B}}$ threshold for the π exchange potential, while no structure for the $\pi\rho\omega$ potential. The existence of this state

TABLE II. Various properties of the $\mathrm{B}^{(*)}\bar{\mathrm{B}}^{(*)}$ bound and resonant states with possible $I^G(J^{PC})$ in $I = 1$. The energies E can be either pure real for bound states or complex for resonances. The real parts are measured from the thresholds as indicated in the second column. The imaginary parts are half of the decay widths of the resonances, $\Gamma/2$. In the last two columns, decay channels of a quarkonium and a light flavor meson are indicated. Asterisk of ρ^* indicates that the decay occurs only with a virtual ρ while subsequently transit to a real photon via vector meson dominance.

$I^G(J^{PC})$	Threshold	E [MeV]		Decay channels	
		π potential	$\pi\rho\omega$ potential	s wave	p wave
$1^+(0^{+-})$	...	...	...	...	$\mathrm{h_b}+\pi$, $\chi_{\mathrm{b}0,1,2}+\rho$
$1^-(0^{++})$	$\mathrm{B}\bar{\mathrm{B}}$	-6.5	no	$\eta_\mathrm{b}+\pi$, $\Upsilon+\rho$	$\mathrm{h_b}+\rho^*$, $\chi_{\mathrm{b}1}+\pi$
$1^+(0^{--})$	$\mathrm{B}\bar{\mathrm{B}}^*$	-9.9	-9.8	$\chi_{\mathrm{b}1}+\rho^*$	$\eta_\mathrm{b}+\rho$, $\Upsilon+\pi$
$1^-(0^{-+})$	$\mathrm{B}\bar{\mathrm{B}}^*$	no	no	$\mathrm{h_b}+\rho$, $\chi_{\mathrm{b}0}+\pi$	$\Upsilon+\rho$
$1^+(1^{+-})$	$\mathrm{B}\bar{\mathrm{B}}^*$	-7.7	-8.5	$\Upsilon+\pi$	$\mathrm{h_b}+\pi$, $\chi_{\mathrm{b}1}+\rho^*$
			$50.4-i15.1/2$		
$1^-(1^{++})$	$\mathrm{B}\bar{\mathrm{B}}^*$	-16.7	-1.9	$\Upsilon+\rho$	$\mathrm{h_b}+\rho^*$, $\chi_{\mathrm{b}0,1}+\pi$
$1^+(1^{--})$	$\mathrm{B}\bar{\mathrm{B}}$	$7.0-i37.9/2$	$7.1-i37.4/2$	$\mathrm{h_b}+\pi$, $\chi_{\mathrm{b}0,1,2}+\rho^*$	$\eta_\mathrm{b}+\rho$, $\Upsilon+\pi$
		$58.8-i30.0/2$	$58.6-i27.7/2$		
$1^-(1^{-+})$	$\mathrm{B}\bar{\mathrm{B}}^*$	no	no	$\mathrm{h_b}+\rho$, $\chi_{\mathrm{b}1}+\pi$	$\eta_\mathrm{b}+\pi$, $\Upsilon+\rho$
$1^+(2^{+-})$	$\mathrm{B}\bar{\mathrm{B}}^*$	no	no	...	$\mathrm{h_b}+\pi$, $\chi_{\mathrm{b}0,1,2}+\rho$
$1^-(2^{++})$	$\mathrm{B}\bar{\mathrm{B}}$	$63.5-i8.3/2$	$62.7-i8.4/2$	$\Upsilon+\rho$	$\mathrm{h_b}+\rho^*$, $\chi_{\mathrm{b}1,2}+\pi$
$1^-(2^{-+})$	$\mathrm{B}\bar{\mathrm{B}}^*$	no	no	$\mathrm{h_b}+\rho$	$\Upsilon+\rho$
$1^+(2^{--})$	$\mathrm{B}\bar{\mathrm{B}}^*$	$2.0-i4.1/2$	$2.0-i3.9/2$	$\chi_{\mathrm{b}1}+\rho^*$	$\eta_\mathrm{b}+\rho$, $\Upsilon+\pi$
		$44.2-i2.5/2$	$44.1-i2.8/2$		

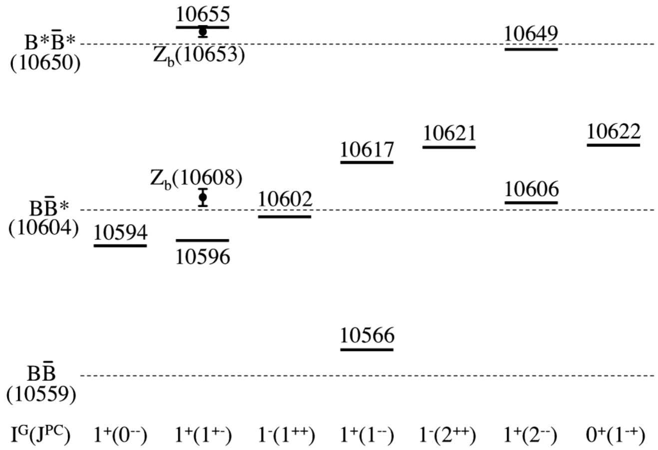

FIG. 1. The $\mathrm{B}^{(*)}\bar{\mathrm{B}}^{(*)}$ bound and resonant states with exotic $I^G(J^{PC})$. The dots with error bars denote the position of the experimentally observed $\mathrm{Z_b}$'s where $M(\mathrm{Z_b}(10\,610)) = 10\,607.2$ MeV and $M(\mathrm{Z_b}(10\,650)) = 10\,652.2$ MeV. Solid lines are for our predictions for the energies of the bound and resonant states when the $\pi\rho\omega$ potential is employed. Mass values are shown in units of MeV.

depends on the details of the potential, while the states in the other quantum numbers are rather robust. Let us see the results for the latter states from the $\pi\rho\omega$ potentials. For $1^+(0^{--})$ and $1^-(1^{++})$, we find bound states with binding energy 9.8 MeV and 1.9 MeV from the $\mathrm{B}\bar{\mathrm{B}}^*$ threshold, respectively. These bound states appear also for the π exchange potential, though the binding energy of the $1^-(1^{++})$ state becomes larger. The $1^-(2^{++})$ state is a resonant state with the resonance energy 62.7 MeV and the decay width 8.4 MeV. The $1^+(1^{--})$ states are twin resonances with the resonance energy 7.1 MeV and the decay width 37.4 MeV for the first resonance, and the resonance energy 58.6 MeV and the decay width 27.7 MeV for the second. The resonance energies are measured from the $\mathrm{B}\bar{\mathrm{B}}$ threshold. The $1^+(2^{--})$ states also form twin resonances with the resonance energy 2.0 MeV and the decay width 3.9 MeV for the first resonance and the resonance energy 44.1 MeV and the decay width 2.8 MeV for the second, where the resonance energies have are measured from the $\mathrm{B}\bar{\mathrm{B}}^*$ threshold.

Next, we discuss the result for the states of isospin $I = 0$. In general, the interaction in these states are either repulsive or only weakly attractive as compared to the cases of $I = 1$. The fact that there are less channel couplings explains less attraction partly. (See also Appendix B.) Because of this, we find only one resonant state with $I^G(J^{PC}) = 0^+(1^{-+})$, as shown in Fig. 1 and in Table III. The $0^+(1^{-+})$ state is a resonant state with the resonance energy 17.8 MeV and the decay width 30.1 MeV for the $\pi\rho\omega$ potential.

In the present study, all the states appear in the threshold regions and therefore are all weakly bound or resonant states. The present results are consequences of unique features of the bottom quark sector; the large reduced mass of the $\mathrm{B}^{(*)}\bar{\mathrm{B}}^{(*)}$ systems and the strong tensor force induced by the mixing of B and B^* with small mass splitting. In fact, in the charm sector, our model does not predict any bound or resonant states in the region where we research numerically. Because the reduced mass is smaller and the mass splitting between D and D^* is larger.

V. EFFECTS OF THE COUPLING TO DECAY CHANNELS

We have employed the hadronic molecular picture and only considered the $\mathrm{B}^{(*)}\bar{\mathrm{B}}^{(*)}$ states so far. In reality, however, the $\mathrm{B}^{(*)}\bar{\mathrm{B}}^{(*)}$ states couple to a bottomonium and a light meson state which is predominantly a pion, as $\mathrm{Z_b}$'s were discovered in the decay channels of $\Upsilon(nS)\pi$ $(n = 1, 2, 3)$ and $\mathrm{h_b}(mP)\pi$ $(m = 1, 2)$ [9,10]. In this section, we estimate the effects of such channel coupling to the $\mathrm{B}^{(*)}\bar{\mathrm{B}}^{(*)}$ states. We give a qualitative estimation for the lowest $\mathrm{B}^{(*)}\bar{\mathrm{B}}^{(*)}$ state in $1^+(1^{+-})$ corresponding to $\mathrm{Z_b}(10\,610)^{\pm}$. Similar effects are expected for other states.

To this purpose, we employ the method of Pennington and Wilson [60]. They calculated charmonium mass shifts for including the effect of open and nearby closed channels and we apply their calculation procedure for $\mathrm{Z_b}$ mass shift. The bare bound state propagator $i/(s - m_0^2)$, where m_0 is the mass of the bare state, is dressed by the contribution of hadron loops $\Pi(s)$. Therefore, the full propagator can be written as

$$G_z(s) = \frac{i}{s - \mathcal{M}^2(s)} = \frac{i}{s - m_0^2 - \Pi(s)} = \frac{i}{s - m_0^2 - \sum\limits_{n=1} \Pi_n(s)}, \tag{29}$$

TABLE III. The $\mathrm{B}^{(*)}\bar{\mathrm{B}}^{(*)}$ bound and resonant states with exotic $I^G(J^{PC})$ in $I = 0$. (Same convention as Table II.).

$I^G(J^{PC})$	Threshold	E [MeV]		Decay channels	
		π potential	$\pi\rho\omega$ potential	s wave	p wave
$0^-(0^{--})$	$\mathrm{B}\bar{\mathrm{B}}^*$	no	no	$\chi_{\mathrm{b1}} + \omega$	$\eta_\mathrm{b} + \omega$, $\Upsilon + \eta$
$0^+(1^{-+})$	$\mathrm{B}\bar{\mathrm{B}}^*$	$28.6 - i91.6/2$	$17.8 - i30.1/2$	$\mathrm{h_b} + \omega^*$, $\chi_{\mathrm{b1}} + \eta$	$\eta_\mathrm{b} + \eta$, $\Upsilon + \omega$
$0^-(2^{+-})$	$\mathrm{B}\bar{\mathrm{B}}^*$	no	no	$\cdots$	$\mathrm{h_b} + \eta$, $\chi_{\mathrm{b0,1,2}} + \omega$

where s is the square of the momentum carried by the propagator. $\mathcal{M}(s)$ is the complex mass function and the real part of this gives the "renormalized" mass. Since the Z_b has five decay channels, the hadron loops $\Pi(s)$ is a sum of each decay channel n (Fig. 2). Each hadron loop $\Pi_n(s)$ (Fig. 2) is obtained by using the dispersion relation in terms of its imaginary part. All hadronic channels contribute to its mass at least in principle. Because the dispersion integral diverges, we have to subtract the square of mass function $\mathcal{M}(s_0)$ at suitable point s_0 from $\mathcal{M}(s)$. We shall discuss the choice of s_0 shortly. Now, we can write the loop function in a once subtracted form as

$$\begin{aligned}\Delta\Pi_n(s, s_0) &\equiv \Pi_n(s) - \Pi_n(s_0)\\ &= \frac{(s-s_0)}{\pi}\int_{s_n}^{\infty} ds' \frac{\mathrm{Im}\Pi_n(s')}{(s'-s)(s'-s_0)}. \end{aligned} \tag{30}$$

Then, we arrive at the mass shift δM as

$$\sum_{n=1}\Delta\Pi_n(s, s_0) = \mathcal{M}^2(s) - m_0^2 \equiv \delta M^2(s). \tag{31}$$

Since an imaginary part of a loop function is proportional to the two-body phase space, we take $\mathrm{Im}\Pi_n$ in the form for $s \geq s_n$ as

$$\mathrm{Im}\,\Pi_n(s) = -g_n^2\left(\frac{2q_{\mathrm{cm}}}{\sqrt{s}}\right)^{2L+1}\exp\left(-\frac{q_{\mathrm{cm}}^2}{\Lambda^2}\right), \tag{32}$$

where g_n is the coupling of Z_b to a decay channel n (a bottomonium and a pion), L is the orbital angular momentum between a bottomonium and a pion. q_{cm} is the magnitude of the three-momentum of a pion in the center-of-mass frame and is related to

$$q_{\mathrm{cm}} = \left(\frac{s + m_\pi^2 - M_{b\bar{b}}^2}{2\sqrt{s}}\right)^2 - m_\pi^2. \tag{33}$$

In Eq. (32), following [60], we have introduced the Gaussian-type form factor with a cutoff parameter Λ which is related to the interaction range R. We set $\Lambda = 600$ MeV as a typical hadron scale; this value corresponds to

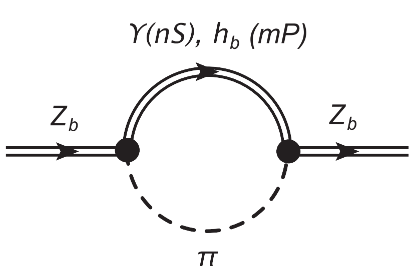

FIG. 2. The diagram corresponding to a loop function $\Pi_n(s)$ of channel n.

TABLE IV. Various contributions to loop corrections of channel n, δM. The total correction is shown on the most right column. The first and the second row show the threshold masses and the coupling strengths of channel n. M_{th} and δM are given in units of MeV.

	$\Upsilon(1S)\pi$	$\Upsilon(2S)\pi$	$\Upsilon(3S)\pi$	$h_b(1P)\pi$	$h_b(2P)\pi$	Total
M_{th}	9600	10 163	10 495	10 038	10 399	...
g_n	1986	844	956	7392	14 179	...
δM	6.3	0.5	−1.3	−0.1	−3.0	2.4

$R \sim 0.8$ fm by using the relation $R \simeq \sqrt{6}/\Lambda$. Coupling g_n is determined from the partial decay width Γ_n, by $\Gamma_n(s) = -\mathrm{Im}\Pi_n(s)/\sqrt{s}$. For the present rough estimation, we postulate that the decay rates for five final states ($\Upsilon(1S)\pi$, $\Upsilon(2S)\pi$, $\Upsilon(3S)\pi$, $h_b(1P)\pi$, $h_b(2P)\pi$) are equal. Then, partial decay width for each decay channel is set as 3 MeV that is one-fifth of the total decay width 15 MeV [9,10].

The subtraction point s_0 determines the renormalization point where the loop correction vanishes. In Ref. [60], the subtraction point was chosen at the mass of J/ψ. Since J/ψ is a deeply bound state of a $c\bar{c}$ pair where the charmonium description works well without a $D\bar{D}$ loop. Now in our situation, there is no such physical bottomonium-like state decaying into a pion and a bottomonium. However, as in the case of J/ψ we expect that the renormalization point of the vanishing loop is located at an energy which is significantly below the thresholods of the particle in the loop. We adopt such an energy at $\sqrt{s_0} = 9000$ MeV, 600 MeV below the $\pi\Upsilon(1S)$, which is similar to the mass difference of J/ψ and $D\bar{D}$.

The resulting mass shift δM due to each coupling is given in Table IV. The total mass shift is $\delta M = 2.4$ MeV, which is slightly repulsive. This means that the mass of the $B^{(*)}\bar{B}^{(*)}$ bound state in $1^+(1^{+-})$ will be pushed up by the $\Upsilon(nS)\pi$ and $h_b(mP)\pi$ couplings. Therefore, we expect that this state gets closer the $B\bar{B}^*$ threshold, or could even become a resonant state. Since the coupling $g_{\Upsilon(1S)\pi}$ is the largest due to its low mass, the largest effect is found for the coupling of $\Upsilon(1S)\pi$, where the mass shift δM is 6.3 MeV. The coupling of $h_b(2P)\pi$ having P-wave contributes attraction, whose mass shift δM is -3.0 MeV. Other coupling channels are minor role.

To summarize this section, we have estimated loop contributions to the mass of the $B^{(*)}\bar{B}^{(*)}$ molecules. We find small repulsive corrections, which still keeps the molecular picture unchanged but may change the bound states into resonances, being consistent with the experimental observation.

VI. SEARCH IN DECAYS FROM $\Upsilon(5S)$

As twin Z_b's were observed from Υ(5S) decay, Υ(5S) decay is a useful source to search the exotic states around the $B^{(*)}\bar{B}^{(*)}$ energy region. Υ(5S) can decay to a

$I^G(J^{PC}) = 1^+(1^{+-})$ state by a single pion emission in s wave, and a $1^+(0^{--})$, $1^+(1^{--})$, or $1^+(2^{--})$ state by a single pion emission in p wave. We recall that the twin $\mathrm{Z_b}$'s with $I^G(J^{PC}) = 1^+(1^{+-})$ were observed in the s-wave channel [9,10]. In the present study, we further predict the bound state in $I^G(J^{PC}) = 1^+(0^{--})$, and new twin resonant states in $I^G(J^{PC}) = 1^+(1^{--})$ and $1^+(2^{--})$ as summarized in Table II. As for the exotic J^{PC} states in isosinglet, the resonant state in $I^G(J^{PC}) = 0^+(1^{-+})$ can be observed from $\Upsilon(5S)$ by ω emission in p wave as shown in Table III.

The radiative decay of $\Upsilon(5S)$ is also an interesting channel as discussed in Ref. [49]. In radiative decay, $\Upsilon(5S)$ decays to the $I^G(J^{PC}) = 1^-(0^{++})$, $1^-(1^{++})$, and $1^-(2^{++})$ states with a photon emission in s wave. These channels can be also produced in hadronic transitions with emission of ρ meson from higher Υ-like bottomonim states. In the present study, we predict the bound states in $I^G(J^{PC}) = 1^-(0^{++})$ and $1^-(1^{++})$ and a resonant states in $1^-(2^{++})$ as summarized in Table II.

As a consequence, we will be able to study the $\mathrm{B}^{(*)}\bar{\mathrm{B}}^{(*)}$ bound and resonant states with positive G parity in a pion emission from $\Upsilon(5S)$ and with negative G parity in a photon emission from $\Upsilon(5S)$. It will be an interesting subject for experiments to search these states in $\Upsilon(5S)$ decays.

VII. SUMMARY

In this paper, we have systematically studied the possibility of the $\mathrm{B}^{(*)}\bar{\mathrm{B}}^{(*)}$ bound and resonant states having exotic quantum numbers $I^G(J^{PC})$. These states are consisted of at least four quarks, because their quantum numbers cannot be assigned by the quarkonium picture and hence they are genuinely exotic states. We have constructed the potential of the $\mathrm{B}^{(*)}\bar{\mathrm{B}}^{(*)}$ states using the effective Lagrangian respecting the heavy quark symmetry. Because of the degeneracy in masses of B and B^* mesons, the channel mixing, such as $\mathrm{B}\bar{\mathrm{B}}^*$-$\mathrm{B}^*\bar{\mathrm{B}}$, $\mathrm{B}^*\bar{\mathrm{B}}^*$-$\mathrm{B}^*\bar{\mathrm{B}}^*$, $\mathrm{B}\bar{\mathrm{B}}$-$\mathrm{B}^*\bar{\mathrm{B}}^*$, and $\mathrm{B}\bar{\mathrm{B}}^*$-$\mathrm{B}^*\bar{\mathrm{B}}^*$, plays an important role to form the $\mathrm{B}^{(*)}\bar{\mathrm{B}}^{(*)}$ bound and/or resonant states. We have numerically solved the Schrödinger equation with the channel couplings for the $\mathrm{B}^{(*)}\bar{\mathrm{B}}^{(*)}$ states with $I^G(J^{PC})$ for $J \le 2$.

As a result, in $I = 1$, we have found that the $I^G(J^{PC}) = 1^+(1^{+-})$ states have a bound state with binding energy 8.5 MeV, and a resonant state with the resonance energy 50.4 MeV and the decay width 15.1 MeV. We have successfully reproduced the positions of $\mathrm{Z_b}(10\,610)$ and $\mathrm{Z_b}(10\,650)$ observed by Belle. Therefore, the twin resonances of $\mathrm{Z_b}$'s can be interpreted as the $\mathrm{B}^{(*)}\bar{\mathrm{B}}^{(*)}$ molecular type states. It should be noted that the $\mathrm{B}\bar{\mathrm{B}}^*$-$\mathrm{B}^*\bar{\mathrm{B}}$, $\mathrm{B}\bar{\mathrm{B}}^*$-$\mathrm{B}^*\bar{\mathrm{B}}^*$, and $\mathrm{B}^*\bar{\mathrm{B}}$-$\mathrm{B}^*\bar{\mathrm{B}}^*$ mixing effects are important, because many structures disappear without the mixing effects. We have obtained the other possible $\mathrm{B}^{(*)}\bar{\mathrm{B}}^{(*)}$ states in $I = 1$. We have found one bound state in each $1^+(0^{--})$ and $1^-(1^{++})$, one resonant state in $1^-(2^{++})$, and twin resonant states in each $1^+(1^{--})$ and $1^+(2^{--})$. It is remarkable that another two twin resonances can exist in addition to the $\mathrm{Z_b}$'s. We have also studied the $\mathrm{B}^{(*)}\bar{\mathrm{B}}^{(*)}$ states in $I = 0$ and found one resonant state in $0^+(1^{-+})$. We have checked the differences between the results from the π exchange potential and those from the $\pi\rho\omega$ potential, and found that the difference is small. Therefore, the one-pion-exchange potential dominates as the interaction in the $\mathrm{B}^{(*)}\bar{\mathrm{B}}^{(*)}$ bound and resonant states.

We have estimated the effects of the coupling to decay channels by means of dispersion relations. Total mass shift is $\delta M = 2.4$ MeV, which is slightly repulsive. Therefore, we conclude that the molecular picture of $\mathrm{B}^{(*)}\bar{\mathrm{B}}^{(*)}$ will be a good approximation for the first step. More systematic analyses will be left for future works.

For experimental studies, the $\Upsilon(5S)$ decay is a useful tool to search the $\mathrm{B}^{(*)}\bar{\mathrm{B}}^{(*)}$ states. $\Upsilon(5S)$ can decay to the $\mathrm{B}^{(*)}\bar{\mathrm{B}}^{(*)}$ states with $1^+(0^{--})$, $1^+(1^{--})$, and $1^+(2^{--})$ by a single pion emission in p wave and the state with $0^+(1^{-+})$ by ω emission in p wave. $\Upsilon(5S)$ can also decay to the $\mathrm{B}^{(*)}\bar{\mathrm{B}}^{(*)}$ states with $1^-(0^{++})$, $1^-(1^{++})$, and $1^-(2^{++})$ by radiative decays. In the future, various exotic states would be observed around the thresholds from $\Upsilon(5S)$ decays in accelerator facilities such as Belle and also would be searched in the relativistic heavy ion collisions in RHIC and LHC [61,62]. If these states are fit in our predictions, they will be good candidates of the $\mathrm{B}^{(*)}\bar{\mathrm{B}}^{(*)}$ molecular states.

ACKNOWLEDGMENTS

We thank Professor S. Takeuchi and Professor M. Takizawa for fruitful discussions and comments. This work is supported in part by Grant-in-Aid for Scientific Research on Priority Areas "Elucidation of New Hadrons with a Variety of Flavors (E01: 21105006)" (S. Y. and A. H.) and by "Grant-in-Aid for Young Scientists (B) 22740174" (K. S.), from the ministry of Education, Culture, Sports, Science and Technology of Japan.

APPENDIX A: HAMILTONIAN

The Hamiltonian is a sum of the kinetic term and potential term as

$$H_{J^{PC}} = K_{J^{PC}} + V^{\pi}_{J^{PC}}, \tag{A1}$$

for the π exchange potential only, and

$$H_{J^{PC}} = K_{J^{PC}} + \sum_{i=\pi,\rho,\omega} V^{i}_{J^{PC}}, \tag{A2}$$

for the $\pi\rho\omega$ potential.

The kinetic terms with including the explicit breaking of the heavy quark symmetry by the mass difference $m_{\mathrm{B}^*} - m_{\mathrm{B}}$ are

$$K_{0^{++}} = \mathrm{diag}\left(-\frac{1}{2\tilde{m}_{\mathrm{BB}}}\triangle_0, -\frac{1}{2\tilde{m}_{\mathrm{BB}^*}}\triangle_0 + 2\Delta m_{\mathrm{BB}^*}, -\frac{1}{2\tilde{m}_{\mathrm{BB}^*}}\triangle_2 + 2\Delta m_{\mathrm{BB}^*}\right), \tag{A3}$$

$$K_{0^{--}} = \mathrm{diag}\left(-\frac{1}{2\tilde{m}_{\mathrm{BB}^*}}\triangle_1\right), \tag{A4}$$

$$K_{0^{-+}} = \mathrm{diag}\left(-\frac{1}{2\tilde{m}_{\mathrm{BB}^*}}\triangle_1, -\frac{1}{2\tilde{m}_{\mathrm{B}^*\mathrm{B}^*}}\triangle_1 + \Delta m_{\mathrm{BB}^*}\right), \tag{A5}$$

$$K_{1^{+-}} = \mathrm{diag}\left(-\frac{1}{2\tilde{m}_{\mathrm{BB}^*}}\triangle_0, -\frac{1}{2\tilde{m}_{\mathrm{BB}^*}}\triangle_2, -\frac{1}{2\tilde{m}_{\mathrm{B}^*\mathrm{B}^*}}\triangle_0 + \Delta m_{\mathrm{BB}^*}, -\frac{1}{2\tilde{m}_{\mathrm{B}^*\mathrm{B}^*}}\triangle_2 + \Delta m_{\mathrm{BB}^*}\right), \tag{A6}$$

$$K_{1^{++}} = \mathrm{diag}\left(-\frac{1}{2\tilde{m}_{\mathrm{BB}^*}}\triangle_0, -\frac{1}{2\tilde{m}_{\mathrm{BB}^*}}\triangle_2, -\frac{1}{2\tilde{m}_{\mathrm{B}^*\mathrm{B}^*}}\triangle_2 + \Delta m_{\mathrm{BB}^*}\right), \tag{A7}$$

$$\begin{aligned} K_{1^{--}} = \mathrm{diag}\Bigg(&-\frac{1}{2\tilde{m}_{\mathrm{BB}}}\triangle_0, -\frac{1}{2\tilde{m}_{\mathrm{BB}^*}}\triangle_1 + \Delta m_{\mathrm{BB}^*}, -\frac{1}{2\tilde{m}_{\mathrm{B}^*\mathrm{B}^*}}\triangle_1 + 2\Delta m_{\mathrm{BB}^*}, \\ &-\frac{1}{2\tilde{m}_{\mathrm{B}^*\mathrm{B}^*}}\triangle_1 + 2\Delta m_{\mathrm{BB}^*}, -\frac{1}{2\tilde{m}_{\mathrm{B}^*\mathrm{B}^*}}\triangle_3 + 2\Delta m_{\mathrm{BB}^*}\Bigg), \end{aligned} \tag{A8}$$

$$K_{1^{-+}} = \mathrm{diag}\left(-\frac{1}{2\tilde{m}_{\mathrm{BB}^*}}\triangle_1, -\frac{1}{2\tilde{m}_{\mathrm{B}^*\mathrm{B}^*}}\triangle_1 + \Delta m_{\mathrm{BB}^*}\right), \tag{A9}$$

$$K_{2^{+-}} = \mathrm{diag}\left(-\frac{1}{2\tilde{m}_{\mathrm{BB}^*}}\triangle_2, -\frac{1}{2\tilde{m}_{\mathrm{B}^*\mathrm{B}^*}}\triangle_2 + \Delta m_{\mathrm{BB}^*}\right), \tag{A10}$$

$$\begin{aligned} K_{2^{++}} = \mathrm{diag}\Bigg(&-\frac{1}{2\tilde{m}_{\mathrm{BB}}}\triangle_2, -\frac{1}{2\tilde{m}_{\mathrm{BB}^*}}\triangle_2 + \Delta m_{\mathrm{BB}^*}, -\frac{1}{2\tilde{m}_{\mathrm{B}^*\mathrm{B}^*}}\triangle_2 + 2\Delta m_{\mathrm{BB}^*}, -\frac{1}{2\tilde{m}_{\mathrm{B}^*\mathrm{B}^*}}\triangle_0 \\ &+ 2\Delta m_{\mathrm{BB}^*}, -\frac{1}{2\tilde{m}_{\mathrm{B}^*\mathrm{B}^*}}\triangle_2 + 2\Delta m_{\mathrm{BB}^*}, -\frac{1}{2\tilde{m}_{\mathrm{B}^*\mathrm{B}^*}}\triangle_4 + 2\Delta m_{\mathrm{BB}^*}\Bigg), \end{aligned} \tag{A11}$$

$$K_{2^{-+}} = \mathrm{diag}\left(-\frac{1}{2\tilde{m}_{\mathrm{BB}^*}}\triangle_1, -\frac{1}{2\tilde{m}_{\mathrm{BB}^*}}\triangle_3, -\frac{1}{2\tilde{m}_{\mathrm{B}^*\mathrm{B}^*}}\triangle_1 + \Delta m_{\mathrm{BB}^*}, -\frac{1}{2\tilde{m}_{\mathrm{B}^*\mathrm{B}^*}}\triangle_3 + \Delta m_{\mathrm{BB}^*}\right), \tag{A12}$$

$$K_{2^{--}} = \mathrm{diag}\left(-\frac{1}{2\tilde{m}_{\mathrm{BB}^*}}\triangle_1, -\frac{1}{2\tilde{m}_{\mathrm{BB}^*}}\triangle_3, -\frac{1}{2\tilde{m}_{\mathrm{B}^*\mathrm{B}^*}}\triangle_1 + \Delta m_{\mathrm{BB}^*}, -\frac{1}{2\tilde{m}_{\mathrm{B}^*\mathrm{B}^*}}\triangle_3 + \Delta m_{\mathrm{BB}^*}\right), \tag{A13}$$

where $\triangle_l = \frac{\partial^2}{\partial r^2} + \frac{2}{r}\frac{\partial}{\partial r} - \frac{l(l+1)}{r^2}$ with integer $l \geq 0$, $1/\tilde{m}_{\mathrm{BB}} = 1/m_{\mathrm{B}} + 1/m_{\mathrm{B}}$, $1/\tilde{m}_{\mathrm{BB}^*} = 1/m_{\mathrm{B}} + 1/m_{\mathrm{B}^*}$, $1/\tilde{m}_{\mathrm{B}^*\mathrm{B}^*} = 1/m_{\mathrm{B}^*} + 1/m_{\mathrm{B}^*}$, and $\Delta m_{\mathrm{BB}^*} = m_{\mathrm{B}^*} - m_{\mathrm{B}}$.

The π exchange potentials for each J^{PC} states are

$$V^{\pi}_{0^{++}} = \begin{pmatrix} 0 & \sqrt{3}V_{\mathrm{C}} & -\sqrt{6}V_{\mathrm{T}} \\ \sqrt{3}V_{\mathrm{C}} & 2V_{\mathrm{C}} & \sqrt{2}V_{\mathrm{T}} \\ -\sqrt{6}V_{\mathrm{T}} & \sqrt{2}V_{\mathrm{T}} & -V_{\mathrm{C}} + 2V_{\mathrm{T}} \end{pmatrix}, \tag{A14}$$

$$V^{\pi}_{0^{--}} = (-V_{\mathrm{C}} - 2V_{\mathrm{T}}), \tag{A15}$$

$$V^{\pi}_{0^{-+}} = \begin{pmatrix} V_{\mathrm{C}} + 2V_{\mathrm{T}} & -2V_{\mathrm{C}} + 2V_{\mathrm{T}} \\ -2V_{\mathrm{C}} + 2V_{\mathrm{T}} & V_{\mathrm{C}} + 2V_{\mathrm{T}} \end{pmatrix}, \tag{A16}$$

$$V^{\pi}_{1^{+-}} = \begin{pmatrix} \mathrm{V_C} & -\sqrt{2}\mathrm{V_T} & -2\mathrm{V_C} & -\sqrt{2}\mathrm{V_T} \\ -\sqrt{2}\mathrm{V_T} & \mathrm{V_C}+\mathrm{V_T} & -\sqrt{2}\mathrm{V_T} & -2\mathrm{V_C}+\mathrm{V_T} \\ -2\mathrm{V_C} & -\sqrt{2}\mathrm{V_T} & \mathrm{V_C} & -\sqrt{2}\mathrm{V_T} \\ -\sqrt{2}\mathrm{V_T} & -2\mathrm{V_C}+\mathrm{V_T} & -\sqrt{2}\mathrm{V_T} & \mathrm{V_C}+\mathrm{V_T} \end{pmatrix}, \tag{A17}$$

$$V^{\pi}_{1^{++}} = \begin{pmatrix} -V_{\mathrm{C}} & \sqrt{2}V_{\mathrm{T}} & \sqrt{6}V_{\mathrm{T}} \\ \sqrt{2}V_{\mathrm{T}} & -V_{\mathrm{C}}-V_{\mathrm{T}} & \sqrt{3}V_{\mathrm{T}} \\ \sqrt{6}V_{\mathrm{T}} & \sqrt{3}V_{\mathrm{T}} & -V_{\mathrm{C}}+V_{\mathrm{T}} \end{pmatrix}, \tag{A18}$$

$$V^{\pi}_{1^{--}} = \begin{pmatrix} 0 & 0 & \sqrt{3}V_{\mathrm{C}} & 2\sqrt{\frac{3}{5}}V_{\mathrm{T}} & -3\sqrt{\frac{2}{5}}V_{\mathrm{T}} \\ 0 & -V_{\mathrm{C}}+V_{\mathrm{T}} & 0 & 3\sqrt{\frac{3}{5}}V_{\mathrm{T}} & 3\sqrt{\frac{2}{5}}V_{\mathrm{T}} \\ \sqrt{3}V_{\mathrm{C}} & 0 & 2V_{\mathrm{C}} & -\frac{2}{\sqrt{5}}V_{\mathrm{C}} & \sqrt{\frac{6}{5}}V_{\mathrm{T}} \\ 2\sqrt{\frac{3}{5}}V_{\mathrm{T}} & 3\sqrt{\frac{2}{5}}V_{\mathrm{T}} & -\frac{2}{\sqrt{5}}V_{\mathrm{C}} & -V_{\mathrm{C}}+\frac{7}{5}V_{\mathrm{T}} & -\frac{\sqrt{6}}{5}V_{\mathrm{T}} \\ -3\sqrt{\frac{2}{5}}V_{\mathrm{T}} & 3\sqrt{\frac{2}{5}}V_{\mathrm{T}} & \sqrt{\frac{6}{5}}V_{\mathrm{T}} & -\frac{\sqrt{6}}{5}V_{\mathrm{T}} & -V_{\mathrm{C}}+\frac{8}{5}V_{\mathrm{T}} \end{pmatrix}, \tag{A19}$$

$$V^{\pi}_{1^{-+}} = \begin{pmatrix} V_{\mathrm{C}}-V_{\mathrm{T}} & -2V_{\mathrm{C}}-V_{\mathrm{T}} \\ -2V_{\mathrm{C}}-V_{\mathrm{T}} & V_{\mathrm{C}}-V_{\mathrm{T}} \end{pmatrix}, \tag{A20}$$

$$V^{\pi}_{2^{+-}} = \begin{pmatrix} V_{\mathrm{C}}-V_{\mathrm{T}} & -2V_{\mathrm{C}}-V_{\mathrm{T}} \\ -2V_{\mathrm{C}}-V_{\mathrm{T}} & V_{\mathrm{C}}-V_{\mathrm{T}} \end{pmatrix}, \tag{A21}$$

$$V^{\pi}_{2^{++}} = \begin{pmatrix} 0 & 0 & \sqrt{3}V_{\mathrm{C}} & -\sqrt{\frac{6}{5}}V_{\mathrm{T}} & 2\sqrt{\frac{3}{7}}V_{\mathrm{T}} & -6\sqrt{\frac{3}{35}}V_{\mathrm{T}} \\ 0 & -V_{\mathrm{C}}+V_{\mathrm{T}} & 0 & -3\sqrt{\frac{2}{5}}V_{\mathrm{T}} & \frac{3}{\sqrt{7}}V_{\mathrm{T}} & \frac{12}{\sqrt{35}}V_{\mathrm{T}} \\ \sqrt{3}V_{\mathrm{C}} & 0 & 2V_{\mathrm{C}} & \sqrt{\frac{2}{5}}V_{\mathrm{T}} & -\frac{2}{\sqrt{7}}V_{\mathrm{T}} & \frac{6}{\sqrt{35}}V_{\mathrm{T}} \\ -\sqrt{\frac{6}{5}}V_{\mathrm{T}} & -3\sqrt{\frac{3}{5}}V_{\mathrm{T}} & \sqrt{\frac{2}{5}}V_{\mathrm{T}} & -V_{\mathrm{C}} & -\sqrt{\frac{14}{5}}V_{\mathrm{T}} & 0 \\ 2\sqrt{\frac{3}{7}}V_{\mathrm{T}} & \frac{3}{\sqrt{7}}V_{\mathrm{T}} & -\frac{2}{\sqrt{7}}V_{\mathrm{T}} & -\sqrt{\frac{14}{5}}V_{\mathrm{T}} & -V_{\mathrm{C}}-\frac{3}{7}V_{\mathrm{T}} & -\frac{12}{7\sqrt{5}}V_{\mathrm{T}} \\ -6\sqrt{\frac{3}{35}}V_{\mathrm{T}} & \frac{12}{\sqrt{35}}V_{\mathrm{T}} & \frac{6}{\sqrt{35}}V_{\mathrm{T}} & 0 & -\frac{12}{7\sqrt{5}}V_{\mathrm{T}} & -V_{\mathrm{C}}+\frac{10}{7}V_{\mathrm{T}} \end{pmatrix}, \tag{A22}$$

$$V^{\pi}_{2^{-+}} = \begin{pmatrix} V_{\mathrm{C}}+\frac{1}{5}V_{\mathrm{T}} & -\frac{3\sqrt{6}}{5}V_{\mathrm{T}} & -2V_{\mathrm{C}}+\frac{1}{5}V_{\mathrm{T}} & -\frac{3\sqrt{6}}{5}V_{\mathrm{T}} \\ -\frac{3\sqrt{6}}{5}V_{\mathrm{T}} & V_{\mathrm{C}}+\frac{4}{5}V_{\mathrm{T}} & -\frac{3\sqrt{6}}{5}V_{\mathrm{T}} & -2V_{\mathrm{C}}+\frac{4}{5}V_{\mathrm{T}} \\ -2V_{\mathrm{C}}+\frac{1}{5}V_{\mathrm{T}} & -\frac{3\sqrt{6}}{5}V_{\mathrm{T}} & V_{\mathrm{C}}+\frac{1}{5}V_{\mathrm{T}} & -\frac{3\sqrt{6}}{5}V_{\mathrm{T}} \\ -\frac{3\sqrt{6}}{5}V_{\mathrm{T}} & -2V_{\mathrm{C}}+\frac{4}{5}V_{\mathrm{T}} & -\frac{3\sqrt{6}}{5}V_{\mathrm{T}} & V_{\mathrm{C}}+\frac{4}{5}V_{\mathrm{T}} \end{pmatrix}, \tag{A23}$$

$$V^{\pi}_{2^{--}} = \begin{pmatrix} -V_{\mathrm{C}}-\frac{1}{5}V_{\mathrm{T}} & \frac{3\sqrt{6}}{5}V_{\mathrm{T}} & -\frac{3\sqrt{3}}{5}V_{\mathrm{T}} & \frac{6\sqrt{3}}{5}V_{\mathrm{T}} \\ \frac{3\sqrt{6}}{5}V_{\mathrm{T}} & -V_{\mathrm{C}}-\frac{4}{5}V_{\mathrm{T}} & -\frac{3\sqrt{2}}{5}V_{\mathrm{T}} & \frac{6\sqrt{2}}{5}V_{\mathrm{T}} \\ -\frac{3\sqrt{3}}{5}V_{\mathrm{T}} & -\frac{3\sqrt{2}}{5}V_{\mathrm{T}} & -V_{\mathrm{C}}-\frac{7}{5}V_{\mathrm{T}} & -\frac{6}{5}V_{\mathrm{T}} \\ \frac{6\sqrt{3}}{5}V_{\mathrm{T}} & \frac{6\sqrt{2}}{5}V_{\mathrm{T}} & -\frac{6}{5}V_{\mathrm{T}} & -V_{\mathrm{C}}+\frac{2}{5}V_{\mathrm{T}} \end{pmatrix}. \tag{A24}$$

The ρ and ω potentials are

$$V^v_{0^{++}} = \begin{pmatrix} V^{v\prime}_{\mathrm{C}} & 2\sqrt{3}V^v_{\mathrm{C}} & \sqrt{6}V^v_{\mathrm{T}} \\ 2\sqrt{3}V^v_{\mathrm{C}} & 4V^v_{\mathrm{C}} + V^{v\prime}_{\mathrm{C}} & -\sqrt{2}V^v_{\mathrm{T}} \\ \sqrt{6}V^v_{\mathrm{T}} & -\sqrt{2}V^v_{\mathrm{T}} & -2V^v_{\mathrm{C}} - 2V^v_{\mathrm{T}} + V^{v\prime}_{\mathrm{C}} \end{pmatrix}, \tag{A25}$$

$$V^v_{0^{--}} = (-2V^v_{\mathrm{C}} + 2V^v_{\mathrm{T}} + V^{v\prime}_{\mathrm{C}}), \tag{A26}$$

$$V^v_{0^{-+}} = \begin{pmatrix} 2V^v_{\mathrm{C}} - 2V^v_{\mathrm{T}} + V^{v\prime}_{\mathrm{C}} & -4V^v_{\mathrm{C}} - 2V^v_{\mathrm{T}} \\ -4V^v_{\mathrm{C}} - 2V^v_{\mathrm{T}} & 2V^v_{\mathrm{C}} - 2V^v_{\mathrm{T}} + V^{v\prime}_{\mathrm{C}} \end{pmatrix}, \tag{A27}$$

$$V^v_{1^{+-}} = \begin{pmatrix} 2V^v_{\mathrm{C}} + V^{v\prime}_{\mathrm{C}} & \sqrt{2}V^v_{\mathrm{T}} & -4V^v_{\mathrm{C}} & \sqrt{2}V^v_{\mathrm{T}} \\ \sqrt{2}V^v_{\mathrm{T}} & 2V^v_{\mathrm{C}} - V^v_{\mathrm{T}} + V^{v\prime}_{\mathrm{C}} & \sqrt{2}V^v_{\mathrm{T}} & -4V^v_{\mathrm{C}} - V^v_{\mathrm{T}} \\ -4V^v_{\mathrm{C}} & \sqrt{2}V^v_{\mathrm{T}} & 2V^v_{\mathrm{C}} + V^{v\prime}_{\mathrm{C}} & \sqrt{2}V^v_{\mathrm{T}} \\ \sqrt{2}V^v_{\mathrm{T}} & -4V^v_{\mathrm{C}} - V^v_{\mathrm{T}} & \sqrt{2}V^v_{\mathrm{T}} & 2V^v_{\mathrm{C}} - V^v_{\mathrm{T}} + V^{v\prime}_{\mathrm{C}} \end{pmatrix}, \tag{A28}$$

$$V^v_{1^{++}} = \begin{pmatrix} -2V^v_{\mathrm{C}} + V^{v\prime}_{\mathrm{C}} & -\sqrt{2}V^v_{\mathrm{T}} & -\sqrt{6}V^v_{\mathrm{T}} \\ -\sqrt{2}V^v_{\mathrm{T}} & -2V^v_{\mathrm{C}} + V^v_{\mathrm{T}} & -\sqrt{3}V^v_{\mathrm{T}} \\ -\sqrt{6}V^v_{\mathrm{T}} & -\sqrt{3}V^v_{\mathrm{T}} & -2V^v_{\mathrm{C}} - V^v_{\mathrm{T}} + V^{v\prime}_{\mathrm{C}} \end{pmatrix}, \tag{A29}$$

$$V^v_{1^{--}} = \begin{pmatrix} V^{v\prime}_{\mathrm{C}} & 0 & 2\sqrt{3}V^v_{\mathrm{C}} & -2\sqrt{\frac{3}{5}}V^v_{\mathrm{T}} & 3\sqrt{\frac{2}{5}}V^v_{\mathrm{T}} \\ 0 & -2V^v_{\mathrm{C}} - V^v_{\mathrm{T}} + V^{v\prime}_{\mathrm{C}} & 0 & -3\sqrt{\frac{3}{5}}V^v_{\mathrm{T}} & 3\sqrt{\frac{2}{5}}V^v_{\mathrm{T}} \\ 2\sqrt{3}V^v_{\mathrm{C}} & 0 & 4V^v_{\mathrm{C}} + V^{v\prime}_{\mathrm{C}} & -\frac{4}{\sqrt{5}}V^v_{\mathrm{C}} & -\sqrt{\frac{6}{5}}V^v_{\mathrm{T}} \\ -2\sqrt{\frac{3}{5}}V^v_{\mathrm{T}} & -3\sqrt{\frac{2}{5}}V^v_{\mathrm{T}} & -\frac{4}{\sqrt{5}}V^v_{\mathrm{C}} & -2V^v_{\mathrm{C}} - \frac{7}{5}V^v_{\mathrm{T}} + V^{v\prime}_{\mathrm{C}} & \frac{\sqrt{6}}{5}V^v_{\mathrm{T}} \\ 3\sqrt{\frac{2}{5}}V^v_{\mathrm{T}} & -3\sqrt{\frac{2}{5}}V^v_{\mathrm{T}} & -\sqrt{\frac{6}{5}}V^v_{\mathrm{T}} & \frac{\sqrt{6}}{5}V^v_{\mathrm{T}} & -2V^v_{\mathrm{C}} - \frac{8}{5}V^v_{\mathrm{T}} + V^{v\prime}_{\mathrm{C}} \end{pmatrix}, \tag{A30}$$

$$V^v_{1^{-+}} = \begin{pmatrix} 2V^v_{\mathrm{C}} + V^v_{\mathrm{T}} + V^{v\prime}_{\mathrm{C}} & -4V^v_{\mathrm{C}} + -V^v_{\mathrm{T}} \\ -4V^v_{\mathrm{C}} + V^v_{\mathrm{T}} & 2V^v_{\mathrm{C}} + V^v_{\mathrm{T}} + V^{v\prime}_{\mathrm{C}} \end{pmatrix}, \tag{A31}$$

$$V^v_{2^{+-}} = \begin{pmatrix} 2V^v_{\mathrm{C}} + V^v_{\mathrm{T}} + V^{v\prime}_{\mathrm{C}} & -4V^v_{\mathrm{C}} + V^v_{\mathrm{T}} \\ -4V^v_{\mathrm{C}} + V^v_{\mathrm{T}} & 2V^v_{\mathrm{C}} + V^v_{\mathrm{T}} + V^{v\prime}_{\mathrm{C}} \end{pmatrix}, \tag{A32}$$

$$V^v_{2^{++}} = \begin{pmatrix} V^{v\prime}_{\mathrm{C}} & 0 & 2\sqrt{3}V^v_{\mathrm{C}} & \sqrt{\frac{6}{5}}V^v_{\mathrm{T}} & -2\sqrt{\frac{3}{7}}V^v_{\mathrm{T}} & 6\sqrt{\frac{3}{35}}V^v_{\mathrm{T}} \\ 0 & -2V^v_{\mathrm{C}} - V^v_{\mathrm{T}} + V^{v\prime}_{\mathrm{C}} & 0 & 3\sqrt{\frac{2}{5}}V^v_{\mathrm{T}} & -\frac{3}{\sqrt{7}}V^v_{\mathrm{T}} & -\frac{12}{\sqrt{35}}V^v_{\mathrm{T}} \\ 2\sqrt{3}V^v_{\mathrm{C}} & 0 & 4V^v_{\mathrm{C}} + V^{v\prime}_{\mathrm{C}} & -\sqrt{\frac{2}{5}}V^v_{\mathrm{T}} & \frac{2}{\sqrt{7}}V^v_{\mathrm{T}} & -\frac{6}{\sqrt{35}}V^v_{\mathrm{T}} \\ \sqrt{\frac{6}{5}}V^v_{\mathrm{T}} & -3\sqrt{\frac{3}{5}}V^v_{\mathrm{T}} & -\sqrt{\frac{2}{5}}V^v_{\mathrm{T}} & -2V^v_{\mathrm{C}} + V^{v\prime}_{\mathrm{C}} & \sqrt{\frac{14}{5}}V^v_{\mathrm{T}} & 0 \\ -2\sqrt{\frac{3}{7}}V^v_{\mathrm{T}} & -\frac{3}{\sqrt{7}}V^v_{\mathrm{T}} & \frac{2}{\sqrt{7}}V^v_{\mathrm{T}} & \sqrt{\frac{14}{5}}V^v_{\mathrm{T}} & -2V^v_{\mathrm{C}} + \frac{3}{7}V^v_{\mathrm{T}} + V^{v\prime}_{\mathrm{C}} & \frac{12}{7\sqrt{5}}V^v_{\mathrm{T}} \\ 6\sqrt{\frac{3}{35}}V^v_{\mathrm{T}} & -\frac{12}{\sqrt{35}}V^v_{\mathrm{T}} & -\frac{6}{\sqrt{35}}V^v_{\mathrm{T}} & 0 & \frac{12}{7\sqrt{5}}V^v_{\mathrm{T}} & -2V^v_{\mathrm{C}} - \frac{10}{7}V^v_{\mathrm{T}} + V^{v\prime}_{\mathrm{C}} \end{pmatrix}, \tag{A33}$$

$$V^v_{2^{-+}} = \begin{pmatrix} 2V^v_C - \frac{1}{5}V^v_T + V^{v\prime}_C & \frac{3\sqrt{6}}{5}V^v_T & -4V^v_C - \frac{1}{5}V^v_T & \frac{3\sqrt{6}}{5}V^v_T \\ \frac{3\sqrt{6}}{5}V^v_T & 2V^v_C - \frac{4}{5}V^v_T + V^{v\prime}_C & \frac{3\sqrt{6}}{5}V^v_T & -4V^v_C - \frac{4}{5}V^v_T \\ -4V^v_C - \frac{1}{5}V^v_T & \frac{3\sqrt{6}}{5}V^v_T & 2V^v_C - \frac{1}{5}V^v_T + V^{v\prime}_C & \frac{3\sqrt{6}}{5}V^v_T \\ \frac{3\sqrt{6}}{5}V^v_T & -4V^v_C - \frac{4}{5}V^v_T & \frac{3\sqrt{6}}{5}V^v_T & 2V^v_C - \frac{4}{5}V^v_T + V^{v\prime}_C \end{pmatrix}, \tag{A34}$$

$$V^v_{2^{--}} = \begin{pmatrix} -2V^v_C + \frac{1}{5}V^v_T + V^{v\prime}_C & -\frac{3\sqrt{6}}{5}V^v_T & \frac{3\sqrt{3}}{5}V^v_T & -\frac{6\sqrt{3}}{5}V^v_T \\ -\frac{3\sqrt{6}}{5}V^v_T & -2V^v_C + \frac{4}{5}V^v_T + V^{v\prime}_C & \frac{3\sqrt{2}}{5}V^v_T & -\frac{6\sqrt{2}}{5}V^v_T \\ \frac{3\sqrt{3}}{5}V^v_T & \frac{3\sqrt{2}}{5}V^v_T & -2V^v_C + \frac{7}{5}V^v_T + V^{v\prime}_C & \frac{6}{5}V^v_T \\ -\frac{6\sqrt{3}}{5}V^v_T & -\frac{6\sqrt{2}}{5}V^v_T & \frac{6}{5}V^v_T & -2V^v_C - \frac{2}{5}V^v_T + V^{v\prime}_C \end{pmatrix}, \tag{A35}$$

where the central and tensor potentials are defined as

$$V^\pi_C = \left(\sqrt{2}\frac{g}{f_\pi}\right)^2 \frac{1}{3} C(r; m_\pi)\vec{\tau}_1 \cdot \vec{\tau}_2, \tag{A36}$$

$$V^\pi_T = \left(\sqrt{2}\frac{g}{f_\pi}\right)^2 \frac{1}{3} T(r; m_\pi)\vec{\tau}_1 \cdot \vec{\tau}_2, \tag{A37}$$

$$V^\rho_C = -(2\lambda g_V)^2 \frac{1}{3} C(r; m_\rho)\vec{\tau}_1 \cdot \vec{\tau}_2, \tag{A38}$$

$$V^\omega_C = (2\lambda g_V)^2 \frac{1}{3} C(r; m_\omega), \tag{A39}$$

$$V^\rho_T = -(2\lambda g_V)^2 \frac{1}{3} T(r; m_\rho)\vec{\tau}_1 \cdot \vec{\tau}_2, \tag{A40}$$

$$V^\omega_T = (2\lambda g_V)^2 \frac{1}{3} T(r; m_\omega), \tag{A41}$$

$$V^{\rho\prime}_C = \left(\frac{\beta g_V}{2m_\rho}\right)^2 \frac{1}{3} C(r; m_\rho)\vec{\tau}_1 \cdot \vec{\tau}_2, \tag{A42}$$

$$V^{\omega\prime}_C = -\left(\frac{\beta g_V}{2m_\omega}\right)^2 \frac{1}{3} C(r; m_\omega). \tag{A43}$$

APPENDIX B: DIAGONALIZATION OF OPEP

We consider the diagonalization of OPEP (A14)–(A24) by adopting a stationary approximation for $B^{(*)}$ and $\bar{B}^{(*)}$ mesons. We regard the $B^{(*)}$ and $\bar{B}^{(*)}$ mesons as sources of isospin, and fix the positions of $B^{(*)}$ and $\bar{B}^{(*)}$ mesons by neglecting the kinetic term. Then, the potentials with channel couplings as matrices in which there are off-diagonal components, turn to be diagonal matrices $\tilde{V}^\pi_{J^{PC}}$ as follows,

$$\tilde{V}^\pi_{0^{++}} = \mathrm{diag}(-3V_C, -V_C + 4V_T, -V_C - 2V_T)\vec{\tau}_1 \cdot \vec{\tau}_2, \tag{B1}$$

$$\tilde{V}^\pi_{0^{--}} = \mathrm{diag}(-V_C - 2V_T)\vec{\tau}_1 \cdot \vec{\tau}_2, \tag{B2}$$

$$\tilde{V}^\pi_{0^{-+}} = \mathrm{diag}(-3V_C, -V_C + 4V_T)\vec{\tau}_1 \cdot \vec{\tau}_2, \tag{B3}$$

$$\tilde{V}^\pi_{1^{+-}} = \mathrm{diag}(3V_C, 3V_C, -V_C + 4V_T, -V_C - 2V_T)\vec{\tau}_1 \cdot \vec{\tau}_2, \tag{B4}$$

$$\tilde{V}^\pi_{1^{++}} = \mathrm{diag}(-V_C + 4V_T, -V_C - 2V_T, -V_C - 2V_T)\vec{\tau}_1 \cdot \vec{\tau}_2, \tag{B5}$$

$$\tilde{V}^\pi_{1^{--}} = \mathrm{diag}(3V_C, -V_C + 4V_T, -V_C + 4V_T, -V_C - 2V_T, -V_C - 2V_T)\vec{\tau}_1 \cdot \vec{\tau}_2, \tag{B6}$$

$$\tilde{V}^\pi_{1^{-+}} = \mathrm{diag}(3V_C, -V_C - 2V_T)\vec{\tau}_1 \cdot \vec{\tau}_2, \tag{B7}$$

$$\tilde{V}^\pi_{2^{+-}} = \mathrm{diag}(3V_C, -V_C - 2V_T)\vec{\tau}_1 \cdot \vec{\tau}_2, \tag{B8}$$

$$\tilde{V}^\pi_{2^{++}} = \mathrm{diag}(3V_C, -V_C - 2V_T, -V_C - 2V_T, -V_C - 2V_T, -V_C + 4V_T, -V_C + 4V_T)\vec{\tau}_1 \cdot \vec{\tau}_2, \tag{B9}$$

$$\tilde{V}^\pi_{2^{-+}} = \mathrm{diag}(3V_C, 3V_C, -V_C - 2V_T, -V_C + 4V_T)\vec{\tau}_1 \cdot \vec{\tau}_2, \tag{B10}$$

$$\tilde{V}^\pi_{2^{--}} = \mathrm{diag}(-V_C - 2V_T, -V_C - 2V_T, -V_C - 2V_T, -V_C + 4V_T)\vec{\tau}_1 \cdot \vec{\tau}_2, \tag{B11}$$

where the central and tensor potentials are defined as $V_C = (\sqrt{2}\frac{g}{f_\pi})^2 \frac{1}{3} C(r; m_\pi)$ and $V_T = (\sqrt{2}\frac{g}{f_\pi})^2 \frac{1}{3} T(r; m_\pi)$, with $V_C > 0$ and $V_T > 0$ and $V_C < V_T$. For $I = 1$ ($\vec{\tau}_1 \cdot \vec{\tau}_2 = 1$), we see that the strongest attractive potential, $-(V_C + 2V_T)$, is contained in the $J^{PC} = 0^{++}, 0^{--}, 1^{+-}, 1^{++}, 1^{--}, 1^{-+}, 2^{+-}, 2^{++}, 2^{-+}$, and 2^{--} states. In another quantum number, the 0^{-+} state in $I = 1$ has only weakly attractive potential, $-3V_C$. Therefore, we expect in $I = 1$ that the $0^{++}, 0^{--}, 1^{+-}, 1^{++}, 1^{--}, 1^{--}, 1^{-+}, 2^{+-}, 2^{++}, 2^{-+}$, and 2^{--} states may be bound and/or resonant states, while the 0^{-+} state hardly forms a structure. For $I = 0$ ($\vec{\tau}_1 \cdot \vec{\tau}_2 = -3$), the strongest attractive potential, $-3 \cdot 3V_C$, is contained in 1^{-+} and 2^{+-} states. The potential in the 0^{--} state is repulsive. Therefore, there may be a bound and/or resonant states in 1^{-+} and 2^{+-}, and no structure in 0^{--} in $I=0$.

Although the static approximation may be a crude approximation, this is a useful method at qualitative level. For example, let us study two nucleon (NN) systems, we analyze the deuteron ($I=0$, $J^P=1^+$) in which the NN potential is given by 2×2 matrix with ${}^3S_1$ and ${}^3D_1$ states [63]. The OPEP for deuteron is given as

$$V^{\pi}_{\mathrm{NN}} = \begin{pmatrix} V^{\mathrm{NN}}_{\mathrm{C}} & 2\sqrt{2}V^{\mathrm{NN}}_{\mathrm{T}} \\ 2\sqrt{2}V^{\mathrm{NN}}_{\mathrm{T}} & V^{\mathrm{NN}}_{\mathrm{C}} - 2V^{\mathrm{NN}}_{\mathrm{T}} \end{pmatrix} \vec{\tau}_1 \cdot \vec{\tau}_2, \tag{B12}$$

with $V^{\mathrm{NN}}_{\mathrm{C}} = (\frac{g_{\pi\mathrm{NN}}}{2m_N})^2 \frac{1}{3} C(r; m_\pi)$ and $V^{\mathrm{NN}}_{\mathrm{T}} = (\frac{g_{\pi\mathrm{NN}}}{2m_N})^2 \frac{1}{3} T(r; m_\pi)$, for a πNN vertex constant $g_{\pi\mathrm{NN}}$ and a nucleon mass m_{N}. We diagonalize Eq. (B12) and obtain the eigenvalues in the diagonal potential,

$$\tilde{V}^{\pi}_{\mathrm{NN}} = \mathrm{diag}(V^{\mathrm{NN}}_{\mathrm{C}} - 4V^{\mathrm{NN}}_{\mathrm{T}}, V^{\mathrm{NN}}_{\mathrm{C}} + 2V^{\mathrm{NN}}_{\mathrm{T}}) \vec{\tau}_1 \cdot \vec{\tau}_2. \tag{B13}$$

Because $V^{\mathrm{NN}}_{\mathrm{T}} > V^{\mathrm{NN}}_{\mathrm{C}}$, the first eigenvalue gives a repulsion in $I=0$, while the second eigenvalue gives an attraction in $I=0$. The eigenvector of the ${}^3S_1$ and ${}^3D_1$ components for the second eigenvalue is $(\sqrt{2/3}, \sqrt{1/3})$. This means that the D-wave probability is about 33 percent. In reality, we have to introduce a kinetic term which disfavors the higher angular momentum (D wave), and hence the D-wave probability in deuteron becomes a few (~ 5) percent. The stationary approximation will be applied to $\mathrm{B}^{(*)}\bar{\mathrm{B}}^{(*)}$ systems with better accuracy, because the B meson mass is 5.6 times larger than the nucleon mass. We note that the OPEPs as a long-range force are better approximation for larger angular momentum, because the sizes of systems are extended. However, the static approximation may become worse for larger angular momentum. Therefore, it is necessary for quantitative analysis to study numerically the solutions of the Schrödinger equations with the kinetic terms and the potentials with channel coupling as discussed in the text.

[1] J. D. Weinstein and N. Isgur, Phys. Rev. D **41**, 2236 (1990).
[2] J. A. Oller and E. Oset, Phys. Rev. D **60**, 074023 (1999).
[3] As a recent review, see T. Hyodo and D. Jido, Prog. Part. Nucl. Phys. **67**, 55 (2012).
[4] N. Brambilla *et al.*, Eur. Phys. J. C **71**, 1 (2011).
[5] N. Brambilla *et al.* (Quarkonium Working Group Collaboration), arXiv:hep-ph/0412158.
[6] E. S. Swanson, Phys. Rep. **429**, 243 (2006).
[7] M. B. Voloshin, Prog. Part. Nucl. Phys. **61**, 455 (2008).
[8] M. Nielsen, F. S. Navarra, and S. H. Lee, Phys. Rep. **497**, 41 (2010).
[9] [B. Collaboration], arXiv:1105.4583.
[10] A. Bondar *et al.* (Belle Collaboration), Phys. Rev. Lett. **108**, 122001 (2012).
[11] N. Isgur and M. B. Wise, Phys. Rev. Lett. **66**, 1130 (1991).
[12] A. V. Manohar and M. B. Wise, Cambridge Monogr. Part. Phys., Nucl. Phys., Cosmol. **10**, 1 (2000).
[13] G. Burdman and J. F. Donoghue, Phys. Lett. B **280**, 287 (1992).
[14] M. B. Wise, Phys. Rev. D **45**, R2188 (1992).
[15] T. M. Yan, H. Y. Cheng, C. Y. Cheung, G. L. Lin, Y. C. Lin, and H. L. Yu, Phys. Rev. D **46**, 1148 (1992); **55**, 5851(E) (1997).
[16] M. A. Nowak, M. Rho, and I. Zahed, Phys. Rev. D **48**, 4370 (1993).
[17] W. A. Bardeen and C. T. Hill, Phys. Rev. D **49**, 409 (1994).
[18] A. M. Badalian, Y. A. Simonov, and M. A. Trusov, Phys. Rev. D **77**, 074017 (2008).
[19] R. Casalbuoni, A. Deandrea, N. Di Bartolomeo, R. Gatto, F. Feruglio, and G. Nardulli, Phys. Rep. **281**, 145 (1997).
[20] W. A. Bardeen, E. J. Eichten, and C. T. Hill, Phys. Rev. D **68**, 054024 (2003).
[21] T. Matsuki, T. Morii, and K. Sudoh, Prog. Theor. Phys. **117**, 1077 (2007).
[22] S. Dubynskiy and M. B. Voloshin, Phys. Lett. B **666**, 344 (2008).
[23] T. E. O. Ericson and G. Karl, Phys. Lett. B **309**, 426 (1993).
[24] N. A. Tornqvist, Phys. Rev. Lett. **67**, 556 (1991).
[25] N. A. Tornqvist, Z. Phys. C **61**, 525 (1994).
[26] I. W. Lee, A. Faessler, T. Gutsche, and V. E. Lyubovitskij, Phys. Rev. D **80**, 094005 (2009).
[27] C. E. Thomas and F. E. Close, Phys. Rev. D **78**, 034007 (2008).
[28] X. Liu, Z. G. Luo, Y. R. Liu, and S. L. Zhu, Eur. Phys. J. C **61**, 411 (2009).
[29] Y. R. Liu, X. Liu, W. Z. Deng, and S. L. Zhu, Eur. Phys. J. C **56**, 63 (2008).
[30] M. Suzuki, Phys. Rev. D **72**, 114013 (2005).
[31] J. R. Zhang, M. Zhong, and M. Q. Huang, Phys. Lett. B **704**, 312 (2011).
[32] D. V. Bugg, Europhys. Lett. **96**, 11002 (2011).
[33] Y. Yang, J. Ping, C. Deng, and H. S. Zong, arXiv:1105.5935.
[34] J. Nieves and M. PavonValderrama, Phys. Rev. D **84**, 056015 (2011).
[35] Z. F. Sun, J. He, X. Liu, Z. G. Luo, and S. L. Zhu, Phys. Rev. D **84**, 054002 (2011).
[36] M. Cleven, F. K. Guo, C. Hanhart, and U. G. Meissner, Eur. Phys. J. A **47**, 120 (2011).
[37] T. Mehen and J. W. Powell, Phys. Rev. D **84**, 114013 (2011).
[38] T. Guo, L. Cao, M. Z. Zhou, and H. Chen, arXiv:1106.2284.
[39] C. Y. Cui, Y. L. Liu, and M. Q. Huang, Phys. Rev. D **85**, 074014 (2012).

[40] F. S. Navarra, M. Nielsen, and J. M. Richard, J. Phys. Conf. Ser. **348**, 012007 (2012).
[41] A. Ali, Proc. Sci., BEAUTY2011 (2011) 002.
[42] M. Karliner, H. J. Lipkin, and N. A. Tornqvist, arXiv:1109.3472.
[43] A. Ali, C. Hambrock, and W. Wang, Phys. Rev. D **85**, 054011 (2012).
[44] D. Y. Chen, X. Liu, and S. L. Zhu, Phys. Rev. D **84**, 074016 (2011).
[45] D. Y. Chen and X. Liu, Phys. Rev. D **84**, 094003 (2011).
[46] D. Y. Chen and X. Liu, Phys. Rev. D **84**, 034032 (2011).
[47] D. Y. Chen, X. Liu, and T. Matsuki, Phys. Rev. D **84**, 074032 (2011).
[48] A. E. Bondar, A. Garmash, A. I. Milstein, R. Mizuk, and M. B. Voloshin, Phys. Rev. D **84**, 054010 (2011).
[49] M. B. Voloshin, Phys. Rev. D **84**, 031502 (2011).
[50] C. Amsler *et al.* (Particle Data Group), Phys. Lett. B **667**, 1 (2008).
[51] H. Y. Cheng, C. Y. Cheung, G. L. Lin, Y. C. Lin, T. M. Yan, and H. L. Yu, Phys. Rev. D **49**, 2490 (1994); C. G. Boyd and B. Grinstein, Nucl. Phys. **B442**, 205 (1995).
[52] H. Ohki, H. Matsufuru, and T. Onogi, Phys. Rev. D **77**, 094509 (2008).
[53] C. Isola, M. Ladisa, G. Nardulli, and P. Santorelli, Phys. Rev. D **68**, 114001 (2003).
[54] S. Yasui and K. Sudoh, Phys. Rev. D **80**, 034008 (2009).
[55] Y. Yamaguchi, S. Ohkoda, S. Yasui, and A. Hosaka, Phys. Rev. D **84**, 014032 (2011).
[56] The $J^{PC} = 0^{+-}$ state cannot be given also in the quarkonium picture.
[57] B. R. Johnson, Chem. Phys. **69**, 4678 (1978).
[58] K. Arai and A. T. Kruppa, Phys. Rev. C **60**, 064315 (1999).
[59] S. Aoyama, T. Myo, K. Kato, and K. Ikeda, Prog. Theor. Phys. **116**, 1 (2006).
[60] M. R. Pennington and D. J. Wilson, Phys. Rev. D **76**, 077502 (2007).
[61] S. Cho *et al.* (ExHIC Collaboration), Phys. Rev. Lett. **106**, 212001 (2011).
[62] S. Cho *et al.* (ExHIC Collaboration), Phys. Rev. C **84**, 064910 (2011).
[63] There is also analysis for $N\bar{N}$ systems in Ref. [64].
[64] C. B. Dover and J. M. Richard, Phys. Rev. D **17**, 1770 (1978).